Studies on the Protection of Arsenic Induced Reproductive Disorders in Adult Male Wistar Rats by Formulated High Protein Diet

Submission of 5000 Words synopsis

SAGNIK BISWAS

Ph.D. registration No.: R-14RS18110014

Date: 6th May, 2016

Supervisor: Prof. Prabir Kumar Mukhopadhyay

Reproductive Toxicology Laboratory

Department of Life Sciences

Presidency University

Kolkata- 700073, West Bengal, India

Synopsis (5000 words)

Name:	Sagnik Biswas
Supervisor:	Prof. Prabir Kumar Mukhopadhyay

Title of Thesis:	Studies on the Protection of Arsenic Induced Reproductive Disorders in Adult Male Wistar Rats by Formulated High Protein Diet
PhD registration Number with date:	R-14RS18110014 dated 5th May, 2016
Enrolment Number with date:	SC/DOC/13-14/33 dated 10th May, 2014
Place of work:	Presidency University, Kolkata
Residential Address:	11/3 Gouri Bari Lane, Kolkata-700004
Corresponding Address:	11/3 Gouri Bari Lane, Kolkata-700004
Email:	sagnik.rs@presiuniv.ac.in
Phone Number:	+91 9903953008

Forwarded

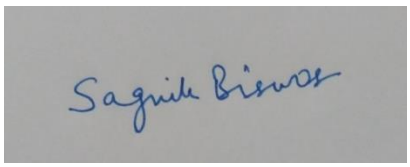

Signature of Research Scholar

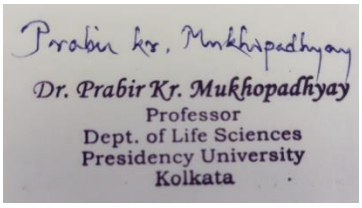

Signature of Supervisor

Contents

Sl. No	Description	Page No
1	Abstract	4
2	Introduction	5-7
3	Aim and Objectives	8
4	Materials and Methods	9-16
5	Results	17-25
6	Discussion	26-31
7	Conclusion	31
8	Significance of this study	32
9	Acknowledgement	32
10	Abbreviations	32-33
11	References	33-38
12	Figures and Tables	39-57
13	Plagiarism Certificate	58
14	Workshop and Conference Certificate attended	59-63
15	Published Manuscript	64-65

Summary of Work

Title- Studies on the protection of arsenic induced reproductive disorders in adult male Wistar rats by formulated high protein diet

1. Abstract

Arsenic toxicity is a major worldwide health problem and has been associated with several reproductive system disorders. The study was designed to investigate the protective role of casein–pea-enriched protein diet /formulated high protein diet (FHPD) on arsenic-mediated testicular and spermatozoal anomalies in adult Wistar rats. The rats (120±10gm) were randomly divided into three groups: Gr I (control) received the normal diet; the Gr II (treated) was given arsenic orally for 30 consecutive days as arsenic trioxide (3mg/kg/rat/day) where as Gr III (supplemented) was given isocaloric FHPD along with arsenic of same dose. Same animal model was used for the fulfillment of all four objectives. The results revealed significant reduction in weight of testis along with other accessory reproductive organs. Structural and functional alterations of testes, cauda epididymis and caudal spermatozoa were observed. Reduction of steroidogenesis and spermatogenesis were also noted. Increased oxidative stress resulted redox imbalance in testes, cauda epididymis and spermatozoa causing successive DNA damages. Apoptosis was initiated in testes as expression of apoptotic markers like Bax, BCl-2, caspase 9 and caspase 3 were seen to be altered. Spermatozoal apoptosis was also noted by Annexin V-Pi staining. Arsenic deposition was also noted in testicular tissues. All these anomalies were attenuated when FHPD supplementation was given to arsenic-gavaged rats. Casein–pea-enriched protein diet mitigated the adverse effects of arsenic and helped in sustaining the normal reproductive functions.

2. Introduction

Arsenic contamination is a serious contemporary toxic hotspot all over the world. Humans are exposed to arsenic mainly through contaminated food and water. Arsenic occurs in the environment as trivalent arsenite (As^{3+}) or pentavalent arsenate (As^{5+}). The maximum permissible level of arsenic in drinking water as set by World Health Organization is 10µg/L or 10ppb [1]. Unfortunately, in the Indian subcontinent, the Ganga-Meghna-Brahmaputra belt is highly affected where in some areas the arsenic contamination of ground water often reaches several hundred times the permissible limit [2]. Acute arsenic exposure includes symptoms of nausea, vomiting with abdominal pain, encephalopathy and neuropathy [3]. Chronic arsenic exposure leads to arsenicosis resulting in pigmentation, keratosis and cancer of skin [4]. However detrimental effects are also observed on cardiovascular, nervous, gastrointestinal, renal, hematological and hepatic systems along with metabolic disorder like diabetes [5]. Reproductive system disorders are also great concern of present day researchers [6].

Arsenic is accredited as a reproductive toxicant in humans [7]. Human populations exposed to arsenic via their occupational exposure, diet and drinking water have been reported with low sperm count, reduced semen quality and infertility [8–10]. In rodents, arsenic toxicity results in weight reduction of testes and other accessory sex organs, inhibition of testicular androgenesis and spermatogenesis, impairment of sperm parameters such as motility, viability [11–13] and count [14]. Alteration in testosterone levels and massive degeneration of germ cells in seminiferous tubules at different stages of development has also been observed [14–17]. Inhibition of testicular function may be due to impaired secretion of pituitary gonadotrophins [11]. Jana et al [11] reported that arsenic exposure disrupts spermatogenesis altering spermatozoal developmental pattern in mice.

Studies have depicted that oxidative stress is the major key player responsible for redox imbalance in reproductive organs like other organs [18–20]. Arsenic possesses electrophilic property by virtue of which it binds to sulfydryl group on proteins causing alteration of its metabolism and thus generates reactive oxygen species (ROS) [21]. Inorganic arsenic in its methylated form reacts with molecular oxygen to produce free radicals (ROS) like, superoxide anion (O^{2-}), hydroxyl radical (OH^{-}), hydrogen peroxide (H_2O_2) singlet oxygen ($_1O^2$) and peroxyl radicals within the cells, specially in the mitochondria [22]. Excessive production of ROS can

not only damage spermatozoal plasma membrane but also causes mitochondrial dysfunction which results the development of infertility in mice [16, 23]. ROS induced Oxidative damages are also responsible base degradation and DNA fragmentation leading to induction of programmed cell death or apoptosis [24, 25]. In brief, ROS disrupts the inner and outer mitochondrial membranes resulting in the release of cytochrome C proteins from the mitochondria and activation of caspases initiating apoptosis [25, 26]. Regulation of the apoptotic pathway occurs via the regulation of proapoptotic and antiapoptotic proteins. The ratio of Bcl-2 to Bax determines the survival or death, following apoptotic stimulation [27]. Taken together, apoptosis is considered to be a key reason for the disruption of spermatogenesis [28].

It seems logical that ROS mediated oxidative stress is one of the important aspect of arsenic toxicity, therefore a therapeutic strategy to increase the antioxidant level of cells is considered important regarding this matter. This purpose might be fulfilled by either removal / prevention of arsenic in interacting with tissues and cellular components or by boosting the cellular antioxidant defense system via exogenous supplementation of antioxidant molecules. Chelation therapy was one of the most extensively used strategies against arsenic toxicity but due to their side effect they were discontinued [29]. With this understanding dietary management seems a logical avenue of research against arsenic threat which included vitamins [30], thiol compounds [31] and micronutrients [29], which have the ability to dislodge toxic metals from tissues and all are unique in one aspect i.e. all are having antioxidant capacity. Various case studies on population depicted that people belonging to poorer strata of the society are the worst sufferer of arsenicosis [32].

In the context of dietary management, pilot studies were done with a diet which contains pea and excess casein against arsenic mediated reproductive disorders in male [33] and female [34] rats from our laboratory. Pea and milk protein casein are known to have anti-oxidant properties and are effective in immunization of lipid peroxidation [35–38]. These proteins also have the ability to prevent free radical-mediated oxidative damages as demonstrated in different liposomal models [35–38]. Pea protein also acts as a potent methyl transferring agent in the methylation process [39] thereby contributing towards detoxification of inorganic arsenic [37]. Arsenic methylation is thus influenced by protein intake and macronutrient status, enhancing dimethyl arsine (DMA) formation and subsequent excretion of arsenic [40, 41]. Further studies have

shown that the diet with high protein (20% more than normal) causes 10-15% increase in urinary arsenic excretion [42]. With this background knowledge, this study focuses the detrimental impacts of arsenic on the male reproductive system concerning testes and epididymal spermatozoa in rat model and exploring the efficacy of a casein–pea-enriched protein diet in ameliorating the toxicities.

3. Aim and Objectives

Whether the dietary modulation i.e. application of casein–pea-enriched protein diet can alleviate arsenic induced male reproductive disorders.

1. To measure the extent of protection by FHPD due to arsenic effect on rat male reproductive system.

2. To determine the extent of oxidative stress by arsenic and its alleviation by FHPD.

3. DNA damage and its reversal upon supplementation.

4. To determine the antiapoptotic action of FHPD.

4. Materials and methods

4.1 Animal selection and treatment

Eighteen adult male albino rats of Wistar strain weighing from 120±10 gm were selected and maintained under standard laboratory conditions (14 hr light: 10 hr dark, 25 ± 2 ˚C temperature) with free access to food and water. The rats were allocated to three groups- Control (Gr-I), Treated (Gr-II) and Supplemented (Gr-III). Aqueous solution of arsenic trioxide at a dose level of 3mg/kg/rat/d [33] was gavaged to treated (Gr-II) and supplemented (Gr-III) rats for 30 consecutive days. The standard diet was composed of 71% carbohydrate, 18% protein, 7% fat, 4% salt mixture and vitamins [34]. This diet was given to rats of Gr-I and Gr-II. Formulated high protein diet (FHPD) [43], which was isocaloric with respect to the normal diet, was prepared by increasing the protein content from 18 to 32% with the addition of 7% pea and 9% excess casein (Table 1) and this particular diet was given to Gr-III rats. During experimentation period behavioral pattern of animals/rats from all groups were noted. Food and water consumption was also monitored.

Similar grouping and treatment schedule were followed in each time to prepare the animal model and subsequent experiments were performed to fulfill the rest of the objectives. Accordingly the same model was prepared for 6 times for achieving the target results from which the experiments were repeated as per their requirement. All the experiments were conducted following the ethical guidelines suggested by the Institutional Animal Ethical Committee and Committee of our University (Sanction number: 796-2011-CPCSEA-PM-SB-22/17-06-15).

4.2 Euthanasia and tissue collection

All the animals were euthanized after 30 days treatment. Immediately serum was separated from blood (using standard protocol), frozen and stored at –20°C for hormonal assays. Organs like testes, epididymis, seminal vesicle and prostate were dissected from each rats and properly weighed. One testis from each group of rat was processed for the histology and SEM analysis, the remaining testis was stored frozen (–80°C) for other studies. Spermatozoa were isolated from cauda epididymis [44] for different studies.

4.3 Body weight and gravimetric index

Initial and final body weight of the rats from all groups was noted. Relative organ weight was calculated from gross organ weight.

4.4 Histology and scanning electron microscopy of testes

For histology, testes from rats of all groups were fixed in Bouin's fixative and embedded in paraffin wax (56–58°C). Five-micrometer thick sections were cut from the middle portion of the testes and stained with routine haematoxylin-eosin (H/E). Same procedure was followed to obtain the stained sections of cauda epididymis.

For scanning electron microscopic (SEM) analysis, rat testes from all groups were fixed, dehydrated and sliced according to the process described by Romero et al. [45], then sputter coated with 5 nm of gold and the images were taken using scanning electron microscope (Zeiss EVO-MA 10).

4.5 Histomorphometry and spermatokinetic analysis

For histomorphometric analysis, at least 40 round seminiferous tubular profiles per animal were measured under high-power objective of a phase-contrast microscope (Zeiss, Thornwood, NY, USA) and subsequently by using Progress Capture Pro 2.5 software (GENOTYPIC Optical Systems GmBH, Jena, Germany). Seminiferous tubule diameter, lumen diameter and seminiferous epithelial height were measured along with Leydig cell and Sertoli cell numbers. Leydig cell nuclear area was also measured. According to the method described by Leblond and Cermount [46] about 40 round tubules per group were randomly selected at 400X magnification for quantification of germ cells. Quantitative evaluation of spermatogonia, preleptotene, pachytene spermatocytes and round spermatids were done in stage VII of seminiferous tubule cycle under 400X magnification. The diameter of nuclei of various germ cell types were measured by using the said software. A correction factor was used to obtain the actual numerical density of germ cells [47].

$$\text{True counts} = \text{crude counts} \times \frac{\text{Section thickness (µm)}}{\text{Section thickness (µm)} + \text{Nuclear diameter (µm)}}$$

4.6 Assessment of spermatozoal potentials and morphology

The cauda epididymis portion was cut and kept in petri-plate containing 2 ml diluents [44] at 37^0C, then an incision was given to allow the sperms to swim out in the medium and from the sperm suspension several studies were carried out.

The sperm suspension (25µl) was transferred into chamber of Neubauer haemocytometer and sperm heads were manually counted [48] using 400X magnification of a phase contrast microscope. This procedure was repeated thrice from each rat in all the groups.

Briefly, 25 µl of the same sperm suspension was kept on a clean slide and then mounted by a cover slip to evaluate the motility study [48] using 400X magnification of a phase contrast microscope. The percentage of sperm motility was categorized in three groups following the literature: progressively motile sperm (PMS), non-progressively motile sperm (NPMS) and non-motile sperm (NMS) according to their motion patterns. This procedure was repeated thrice from each rat in all the groups.

Assessment of sperm viability was carried out by Eosin-Nigrosin staining [48]. In short, 40µl sperm suspension was transferred to an eppendorf and 40µl of EosinY and Nigrosin were added separately and mixed well. Thin smears were then prepared on clean 4 grease free slides, dried and observed under a light microscope at 400X magnification. Viable sperm remained colorless while nonviable sperm stained red/pink and their percentage was estimated. From 1 control rat 4 slides were counted and average data was presented as a single set of data and respectively rest 5 data were calculated from the other 5 control rats. Similarly this procedure was repeated in other groups of rats.

The eosin-nigrosin stained sperm smears (4 slides per animal in each group) were also used to evaluate sperm morphology under 400X magnification of a phase contrast microscope to detect sperm abnormalities. From 1 control rat 4 slides were counted and average data was presented as a single set of data and respectively rest 5 data were calculated from the other 5 control rats. Similarly this procedure was repeated in other groups of rats.

Functional integrity of sperm plasma membrane was carried out by hypo-osmotic swelling test (HOST) [49]. Briefly 0.1 ml of the said sperm suspension was kept in 1.0 ml of hypo-osmotic solution and incubated for 30-60 mins at 37°C and after that spermatozoa were observed under 400X magnification of a phase contrast microscope. HOS positive spermatozoa represented a

curly tail and their percentage was calculated. This procedure was repeated thrice from each rat in all the groups.

4.7 Electron microscopy of spermatozoa

Scanning Electron Microscopy on spermatozoa morphology was done following the protocol of [50]. In brief, the caudal spermatozoal suspension was fixed in 2.5% buffered glutaraldehyde for one hour and then smeared on clean cover slip. Later the dried sperm were sputter coated with gold and observed under scanning electron microscope (Zeiss EVO-MA 10). From 1 control rat 4 coverslips were counted and average data was presented as a single set of data and respectively rest 5 data were calculated from the other 5 control rats. Similarly this procedure was repeated in other groups of rats.

4.8 Steroidogenic activity

The activities of two important key steroidogenic regulatory enzymes *i.e.* Δ^5,3β-hydroxysteroid dehydrogenase (HSD) [51] and 17β-HSD [52] were evaluated by spectrophotometer at 340 nm respectively from the testicular homogenates. This was done in triplicate from each rat which was averaged to get 1 data. Accordingly 5 data were obtained from rest 5 rats of each group.

The testosterone level was assessed from the isolated serum samples by using an enzyme-linked immunosorbent assay (ELISA) kit (Accu Bind, Monobind Inc, USA). The optical density was measured at 450 nm with an ELISA reader (Multiskan, Thermo Lab Systems, Franklin, MA, USA). The intra-assay and inter-assay variations were found to be <7.3% and <6.0%, respectively, and the sensitivity of detection for testosterone was 0.05 ng/ml.

4.9 Assessment of testicular special functional markers

The activity of testicular acid phosphatase (ACP) [53] and alkaline phosphatase (ALP) [54] were measured following the standard protocol. Testicular lactate dehydrogenase and γ-glutamyl transferase activities were measured using the kit purchased from span diagnostics (Mumbai, India). Triplicate assay was done from each rat and the total experimental and calculation was done following the procedure as mentioned earlier.

4.10 Oxidative stress assessment in testes and cauda epididymis

Oxidative stress was determined by biochemical evaluation of the following spectrophotometric analysis of non-enzymatic and enzymatic parameters. Lipid peroxidation (LPO) was assessed by

measuring the fluorescent red adduct as formed by the reaction of thiobarbituric acid (TBA) with malondialdehyde (MDA) (due to oxidation of omega-3 and omega-6 fatty acids) [55]. Protein carbonyl (PC) content of the testicular tissue homogenate formed due to protein oxidation was measured following a reaction with 2,4-dinitrophenylhydrazine (DNPH) [56]. Reduced glutathione (GSH) content of the testicular tissue was measured by the reaction catalyzed by the reduction of 5,5-dithiobis-2-nitrobenzoate to 2-nitro-5-thiobenzoate [57]. Superoxide dismutase (SOD) activity was determined following autoxidation of hematoxylin according to the method developed by Martin et al. [58]. The catalase activity was assessed spectrophotometrically following the catalytic breakdown of H_2O_2 by catalase [59]. The GST assay was assessed based on its catalyzing effect on the conjugation reaction with glutathione as described by Boyland et al. [60]. The activity of the enzyme GPx was measured according to the method of Flohe and Gunzler [61]. GR activity was measured according to the method of Smith et al [62]. Each enzymatic assay was repeated thrice from each rat in all the groups.

4.11 DNA fragmentation assay

DNA from testes and cauda epididymis were extracted by phenol/chloroform-/isoamyl alcohol by following a standard protocol [63, 64]. The purity of the extracted DNA was determined by assessment of the ratio of the absorbance at 260/280 nm. Then 3µg of DNA per sample were loaded along with a DNA marker (standard) into 0.8% agarose gel with ethidium bromide. The samples were run at 5V for 5 minutes followed by increasing to 100V and finally documented in the gel documentation system (Bio-Rad).

4.12 Spermatozoal ROS generation assay by DCFDA (2,7-dichlorofluorescin)

Intracellular H_2O_2 levels in the cauda epididymal spermatozoa were assessed using a fluorescent probe, DCFH-DA. The sperm cells were adjusted to one million per ml and DCFDA dissolved in DMSO was added to 5 mM final concentration. The samples were stored in dark for 30 min and the samples were analyzed on a flow cytometer (BD Accuri C6). FL1 channel was used to collect the DCFDA signal.

4.13 Evaluation of sperm maturity and DNA integrity

Sperm maturity was evaluated by assessing the histone and protamine contents of the sperm nuclei by aniline blue (AB) staining [65]. The histone-rich nuclei of immature spermatozoa

reacted positively by taking up the aniline blue stain and turned blue, whereas the protamine-rich nuclei of mature spermatozoa remained non-reactive and thus unstained. The percentage of blue-stained (AB+ve) and unstained (AB-ve) spermatozoa were calculated under a phase contrast microscope.

Spermatozoa DNA integrity was assessed by staining the air-dried sperm smears with acridine orange (AO) dye following the protocol of Tejada et al. [66]. Spermatozoa with native double-stranded DNA fluoresced green whereas those with denatured DNA fluoresced yellow to red due to meta-chromatic shifting. The percentage of intact native DNA with relation to the denatured one was calculated under a fluorescent microscope (AXIO Imager M1 fluorescence microscope, Carl Zeiss, Germany).

The alkaline comet assay of spermatozoa was performed following the method of Trivedi PP et.al [67]. The fluorescent labeled DNA was visualized using an AXIO Imager M1 fluorescence microscope (Carl Zeiss, Germany) and the resulting images from the slides of all the samples were captured on a computer and processed with COMET SCORE software (TriTek Corp., Sumerduck, VA, USA).

4.14 Spermatozoal apoptosis estimation

Flow cytometry measures apoptosis and phosphatidylserine (PS) translocation across the plasma membranes [68, 69]. FITC Annexin V/Dead Cell Apoptosis Kit (Invitrogen) was used to detect the translocation of PS and type of cell death on epididymal spermatozoa of control, arsenic treated and FHPD supplemented rats. As soon as possible, the stained cells were analyzed by flow cytometry (BD Accuri C6) and the fluorescence emission was measured at 530 nm and > 575 nm.

4.15 RNA extraction and cDNA synthesis

RNA was extracted from testicular tissue (frozen by liquid nitrogen) by Trizol, after that it was mixed with phenol and chloroform and centrifuged at 13000g. RNA pellet was washed with cold ethanol, air dried and dissolved in 1X TAE buffer. The quality of the extracted RNA was evaluated with a spectrophotometer (NanoDrop ND-2000, USA), and only a pure RNA sample with an A260/A280 ratio of 1.8:2 was used for cDNA synthesis, which was performed using 1 µg of RNA and first strand cDNA synthesis kit following the manufacturer's instructions

(Biobharti Pvt. Ltd., India). The synthesized cDNA was stored at −80 °C for subsequent investigations.

4.16 Real-time PCR using SYBER Green

Quantitative real-time PCR was performed using the Bio-Rad CFX96 (C1000) Touch Real-time PCR (Bio-Rad, USA). The relative quantification was performed by determining the increase in the fluorescence light associated with the SYBR Green bonding. Quantitative real-time PCR performed according to the protocol of Mahadevi S [70] with some modifications. Quantitative real-time PCR performed in 10 µl, included in 1.5 µl of cDNA, 5 µl of SYBR Green Master Mix, 2 µl of primer (1 µl forward and 1 µl reverse) and 1.5 µl of deionized water. The Primer3 tool (NCBI-NIH) was used for primer designing of Bax, Bcl-2 and β-actin (Table 2). The amplification conditions and thermal cycle for Bax, Bcl-2 and β-actin were as follows: initial denaturation at 95 °C for 5 seconds followed by 40 cycles at 61 °C for 30 seconds and a final extension at 75 °C for 20 seconds. All the experiments were performed many times in order to ensure reproducibility. The relative expression levels of mRNAs were calculated using the ΔΔCt method. The relative fold increase was also calculated using the following equation:

$RFI = 2^{-\Delta\Delta CT}$.

4.17 Immunoblotting of apoptotic protein markers from testes

The immune blots from isolated testicular tissue samples from different animal groups were prepared according to the protocol of [43] with slight modifications. Blots were subsequently incubated overnight at 4 °C with rabbit anti-Bax, anti-BCl2 (Biobharti Pvt. Ltd., India), anti-caspase-3, anti-caspase-9 (Cell signalling technology, USA) antibodies at 1:1000 dilutions. Rabbit anti-β-actin (Biobharti Pvt. Ltd., India) was used at 1:1000 dilutions as a loading control. Upon washing, blots were subsequently incubated with alkaline phosphatase-conjugated anti-rabbit IgG secondary antibody at 1:2000 dilutions for 1 h at 25 °C. Immunoreactive proteins were detected by staining the membranes with NBT-BCIP (Promega) substrate solution. Intensities of the bands were measured by ImageJ (NIH, USA; Version 1.52a) software. The mean pixel intensity was normalized to the corresponding β-actin and average of each replicate (n = 6) was thereby calculated. The relative concentration of each protein was calculated taking that of control to be one [71].

4.18 Total arsenic estimation from testes

Arsenic concentration was estimated by sample digestion technique followed by atomic absorption spectrometry according to the standard protocol as described by Chowdhury et. al [72]. In brief, wet testicular tissues (.05 gm) were digested in teflon bomb with 2:1 nitric acid and hydrogen peroxide for 10 min 90°C. Digested samples were air dried overnight at hot air oven at 120°C. For evaporation, samples were placed on hotplate at 90°C and final sample volume was adjusted up to 30 ml with ethanol and absorption was measured using atomic absorption spectroscopy (FI-HG-AAS- AA 140 AAS-USA).

4.19 Statistical analysis

The data are presented as the mean ± standard error of the mean (SEM). One-way ANOVA followed by Tukey's HSD post hoc analysis was performed to check any statistical difference between the parameters of the studied groups and $p<0.05$ was considered as lowest significant. Statistical analysis was carried out using the statistical program packages SPSS version 20.0 (SPSS Inc., Chicago, USA).

5. Results

Objective 1

To fulfill the first objective, studies like histology, histomorphometry, ultrastructural analysis of testes and spermatozoa, assessment of potentials and morphology of spermatozoa were carried out. The subsequent results are presented here.

5.1.1 Behavioral pattern along with food and water intake

Consumption of food and intake of water were analogous in rats of all groups. Aggressiveness was seen to develop in arsenic treated rats in the last phase of treatment. Loss of hair was also noted in the same group.

5.1.2 Role of FHPD on body weight, organ weight and gravimetry in arsenic exposed rats

No change of body weight of rats between-the-groups was noted. However, arsenic treatment caused marked reduction in the weight of testis, epididymis, seminal vesicle, and prostate as calculated directly from organ weight and also by gravimetry ($p<0.001$ in all the cases respectively) (Table 3). Supplementation of FHPD resulted significant protection ($p<0.001$) but it was not upto the control level ($p<0.001$ in both the cases) (Table 3).

5.1.3 Effect of FHPD on testicular histology and histomorphometry in arsenic intoxicated rats

Well organized seminiferous tubules were seen in the testicular sections of control rats (Figure 1a & 1d). Analysis of the sections from arsenic group revealed haphazard orientation, loosely packed and partially depleted spermatogenic cells in seminiferous tubule (Figure 1b & 1e). The other visible differences were reduction of sperm population in the luminal area and the presence of vacuoles in the germinal epithelium (Figure 1b & 1e). All these alterations were almost absent in the FHPD supplemented rats (Figure 1c & 1f).

Histomorphometric analysis not only confirmed a robust reduction of mean seminiferous tubular diameter ($p<0.001$) but also showed a successive decrease of germinal epithelial height ($p<0.001$) accompanied with enlarged luminal diameter ($p<0.001$) in arsenic exposed rats (Table 4). FHPD supplementation alleviated all these alterations ($p<0.01$, $p<0.01$ & $p<0.001$ respectively) but dissimilarities existed in germinal epithelial height ($p<0.001$) and lumen diameter ($p<0.01$) with accordance to that of control group (Table 4). Reduction in Leydig cell

population ($p<0.001$), Leydig cell nuclear area (LCNA) ($p<0.001$) and Sertoli cell number ($p<0.001$) were also observed (Table 4). All the changes were not seen ($p<0.001$ in all the cases) in FHPD supplemented group though significant difference ($p<0.01$) existed in LCNA with reference to that of control (Table 4).

5.1.4 Role of FHPD on ultrastructure of testes in arsenic exposed state

Scanning electron microscopic images of testis from control rat demonstrated evenly distributed seminiferous tubules consisting properly oriented spermatogenic cells along with regularly arranged basement membrane (Figure 2a). Arsenic toxicity caused degeneration of the seminiferous lining, disoriented spermatogenic cells and irregular basement membranes (Figure 2b). The changes were almost absent in FHPD supplemented group (Figure 2c).

5.1.5 Role of FHPD supplementation on spermatozoal features under arsenic induced state

The number of spermatozoa isolated from cauda was seen to be decreased ($p<0.001$) in arsenic-induced rats which was also seen to be recovered upon supplementation ($p<0.001$) though difference persisted with that of normal rats ($p<0.001$) (Table 5). Reduction of PMS ($p<0.001$) along with increase in NPMS ($p<0.001$) and NMS ($p<0.001$) were noted in treated group (Table 5). This consequence led to decrease ($p<0.001$) in TMS *i.e.* the summation of PMS+NPMS, in comparison to control rats. All the changes were seen to be mitigated upon FHPD supplementation ($p<0.001$ in all cases) but differences still existed with those of normal rats ($p<0.001$ in all cases) (Table 5). Decline in percentage of viable spermatozoa due to the treatment was noted ($p<0.001$) which reverted back to near normal upon the FHPD application ($p<0.001$) but difference was still there with the values found in control rats ($p<0.001$) (Table 5). The assessment of spermatozoal tail membrane integrity through HOS test showed that the presence of HOS^{+ve} spermatozoa decreased ($p<0.001$) due to arsenic effect but improvement was noticed when supplementation was given ($p<0.001$) though a significant number of spermatozoa ($p<0.001$) still remained affected (Table 5).

5.1.6 Role of FHPD on spermatozoal morphology in arsenic intoxicated rats

Eosin/Nigrosin stained spermatozoa was not only used for viability (live or dead) assessment (Figure 3a) but also demonstrated structural anomalies with respect to normal spermatozoa (Figure 3b). Structural changes of spermatozoa have been categorized as primary and secondary

defects, and Table 6 represents their relative occurrence (in percentage) among different groups. Arsenic exposure caused more secondary defects (Figure 3d-i) compared to the primary defect (Figure 3c) and ultimately caused an overall increase ($p<0.001$) of the total population of abnormal spermatozoa (Table 6). The incidence of such anomalies was found in the FHPD group also ($p<0.001$) but with lesser frequencies.

5.1.7 Effect of FHPD on spermatozoal ultrastructure in arsenic induced state

The SEM images also attested the occurrence of the same type of anomalies on spermatozoal structure in the arsenic-treated group (Figure 4b-h) with respect to normal spermatozoa (Figure 4a). The structural irregularities of spermatozoa were also present in the FHPD group but at reduced rate.

5.1.8 Effect of FHPD on spermatozoal head ultrastructure in arsenic exposed rats

The sperm head region of control rat showed the standard features like intact perforatium (sub-acrosomal material), adequately covered acrosome by an intact acrosomal membrane followed by plasma membrane, prominent post-nuclear cap and post-acrosomal dense lamina (Figure 5a). The spermatozoa from the arsenic-exposed rat (Figure 5b) demonstrated acute dorsoventral constriction in the mid-region with bulged perforatium and disappearance of the post-nuclear cap with serrations. There was interruption of the plasma as well as the acrosomal membrane. The length of the post-acrosomal dense laminar region was shortened with altered shape and size (Figure 5b). These changes were there in the spermatozoa from the FHPD-administered rats also but with lesser incidence (Figure 5c). As presented in Table 7, the incidence of head deformity (%) was significantly higher ($p<0.001$) in the arsenic-treated group, as compared to those of control and FHPD-fed groups. Although FHPD significantly ($p<0.001$) protected the spermatozoa against these arsenic-induced damages, a total protection was not attained (Gr-I vs. Gr-III: $p<0.001$).

Objective 2

To fulfill the second objective the following experiments were performed which included spermatokinetic study, assessment of testicular markers, steroidogenic activity, testicular oxidative stress measurement and testicular DNA fragmentation study. The subsequent results are presented here.

5.2.1 Role of FHPD on spermatogenic growth pattern in arsenic induced state

The spermatokinetic analysis at stage VII of seminiferous epithelial cycle of rats from all groups was done (Figure 6 a & b). The quantitative study of the cells of seminiferous tubules of arsenic treated rats exhibited that the numbers of SgA ($p<0.001$), pLSc ($p<0.001$), mPSc ($p<0.001$) and 7Sd ($p<0.001$) were diminished showing overall spermatogenic arrest as compared to control group (Table 8). However, subsequent FHPD supplementation augmented their numbers [($p<0.001$), ($p<0.01$), ($p<0.01$), ($p<0.001$) respectively] although significant differences [($p<0.01$), ($p<0.01$), ($p<0.01$), ($p<0.001$) respectively] still existed with control group (Table 8). As per the literature the ratio of mPSc to 7Sd should be 1:4 which is indicative of normal spermatogenic development. In this study the ratio was found to be 1:3.11 in arsenic treated group, where as 1:3.48 and 1:3.39 were the respective values in control group and in FHPD supplemented group (Table 8). The spermatid degeneration in arsenic exposed group after calculation from the above ratio was found to be 28.38% i.e. very high in comparison to that of control (14.91%), indicating marked developmental arrest at the late stage of spermatcytogenesis. Eventually, the degree of spermatid degeneration was seen to be lesser in FHPD administered group (18.47%). Thus, the effective 7Sd degeneration observed in arsenic and FHPD groups were +13.47 and +3.56 respectively compared to that of control group (Table 8).

5.2.2 Role of FHPD on the activities of testicular marker enzymes in arsenic exposed state

The activities of testicular LDH, ACP, ALP and γ-GT are essential for normal spermatogenic growth and maintenance and thus considered as essential functional markers. Here the activities of LDH, ACP and ALP were assessed from all groups and it was observed that the treatment caused significant increase ($p<0.001$ in all the cases respectively) with respect to those of control (Table 9). However, the γ-GT activity was significantly reduced ($p<0.001$) following arsenic exposure (Table 9). FHPD supplementation significantly restored the activity of all the enzymes

although significant differences [($p<0.001$), ($p<0.001$), ($p<0.001$), ($p<0.001$) respectively] still persisted with that of control group (Table 9).

5.2.3 Effect of FHPD on testicular steroidogenic activity in arsenic exposed state

Arsenic toxicity caused a noticeable decrease in the activities of testicular Δ^5, 3β-HSD and 17β-HSD ($p<0.01$ and $p<0.05$ respectively) and the level of testosterone ($p<0.001$), as compared to those of control rats (Table 10). FHPD could efficiently prevent these adverse effects of arsenic and maintained the enzyme activities and testosterone level as same as those of control rats.

5.2.4 Role of FHPD on testicular oxidative balance in arsenic induced rats

Oxidative balance is maintained by regulation of both non-enzymatic and enzymatic markers.

5.2.4.1 Non-enzymatic markers

As compared to the control group, the arsenic-exposed rats had significantly higher levels of testicular MDA ($p<0.001$) and PC content ($p<0.001$) and reduced content of GSH ($p<0.01$) (Table 11). In the FHPD-fed group, the MDA level ($p<0.001$) and the GSH content ($p<0.001$) were maintained at the control levels (Table 11). Even though FHPD significantly lowered PC content ($p<0.001$) but it was not upto the control value ($p<0.001$) (Table 11).

5.2.4.2 Enzymatic markers

Arsenic exposure trimmed down the activities of SOD ($p<0.001$), catalase ($p<0.001$), GST ($p<0.001$), GPx ($p<0.001$) and GR ($p<0.001$) reflecting a state of triggered testicular oxidative stress (Table 12). FHPD supplementation potentially protected the testis from the arsenic effects. FHPD maintained the activities of SOD, catalase, GST, GPx, GR to near normal levels [($p<0.001$), ($p<0.001$), ($p<0.001$), ($p<0.001$), ($p<0.001$) respectively], however significant difference still persisted in case of catalase ($p<0.001$) with control group (Table 12).

5.2.5 Effect of FHPD on testicular DNA status in arsenic exposed state

Investigation of isolated testicular DNA from the rats of all groups by using agarose gel electrophoresis revealed that the existence of fragmented DNA in arsenic exposed group (Figure 7). High molecular weight single band DNA were seen in all groups however a prominent ladder

pattern was seen only in arsenic intoxicated group suggesting DNA strand breakage as evidenced by the presence of low molecular weight fragments of DNA (Figure 7).

Objective 3

To accomplish the third objective the following studies were performed which included histology of cauda epididymis, measurement of cauda epididymal oxidative stress, DNA fragmentation of cauda epididymis; spermatozoal DNA integrity, maturity, damage and ROS production. The subsequent results are presented here.

5.3.1 Effect of FHPD on cauda epididymal histology in arsenic induced state

Transverse section of cauda epididymal tubules of control rat showed intact pseudo-stratified columnar epithelium, presence of stereocilia and lumen filled with spermatozoa (Figure 8a & d). On the other hand, arsenic exposure resulted in thinning of pseudo-stratified columnar epithelium, decrease in stereocilia and presence of fewer spermatozoa in the lumen of cauda epididymis (Figure 8b & e). FHPD supplementation restored the epididymal changes inspite of arsenic exposure (Figure 8c & f).

5.3.2 Role of FHPD on oxidative balance of cauda epididymis under arsenic stress

Arsenic exposure in cauda epididymis resulted in marked increase in the levels of MDA ($p<0.001$) and PC content ($p<0.001$) along with reduction in enzymatic activities of SOD ($p<0.001$) and catalase ($p<0.001$) when compared to those from untreated cauda epididymis (Table 13). Eventually in FHPD supplemented group protection was observed ($p<0.001$ in all cases) as the values were noted to near normal (Table 13).

5.3.3 Role of FHPD on epididymal DNA status in arsenic exposed condition

Fragmentation of cauda epididymal DNA was observed in arsenic treated group (Figure 9). Single band DNA of high molecular weight was observed in all groups, yet eminent low molecular weight DNA fragments was noted in arsenic group (Figure 9). Protection was observed in FHPD administered group as no indication of DNA fragments was found (Figure 9).

5.3.4.1 Effect of FHPD on caudal spermatozoal maturity and DNA status in arsenic exposed rats

Studies with AO staining of spermatozoa from all groups (Figure 10a-c) were critically assessed. Arsenic treatment markedly increased ($p<0.001$) the percentage of sperm DNA damage as evidenced by metachromatic shifting from green to red fluorescence (Table 14). A significant ($p<0.001$) prevention of such damage was articulated in the FHPD-fed group, although the incidence of DNA damage still remained higher ($p<0.001$) than that of the control group (Table 14). In the other experiment, as opposed to the control group, the arsenic-treated rats exhibited a significantly higher proportion of AB+ve (Figure 10d) spermatozoa ($p<0.001$). The relative occurrence of AB+ve spermatozoa was considerably lower in the FHPD-fed group ($p<0.001$); however, it remained higher as compared to the control group ($p<0.001$) (Table 14).

5.3.4.2 Role of FHPD on caudal spermatozoal DNA damage under arsenic stress

Arsenic treatment led to decrease in percentage of head DNA of caudal spermatozoa ($p<0.001$) and associated increase in tail DNA percentage ($p<0.001$) when compared to those from control group (Figure 11 c & d) (Table 15). As a result tail movement (%) and olive tail movement (%) were seen to be increased ($p<0.001$ and $p<0.05$) with respect to control group (Table 15). In FHPD supplemented group percent head DNA was increased ($p<0.001$) with a concomitant decrease in percent tail DNA ($p<0.001$), percent tail movement ($p<0.01$) and percent olive tail movement ($p<0.05$) with those of arsenic treated group (Figure 11 e & f) (Table 15).

5.3.5 Effect of FHPD on ROS generation in caudal spermatozoa under arsenic insult

Arsenic ingestion significantly increased ($p<0.001$) spermatozoal ROS to a higher extent (Figure 12). However, in FHPD supplementation restrained spermatozoal ROS generation ($p<0.001$) and maintained to near normal values (Figure 12).

Objective 4

To attain the fourth objective the following experiments were accomplished which included testicular mRNA level expression of Bax and BCl-2, testicular protein expression of Bax and BCl-2, testicular protein expression of caspase 9 and caspase 3, spermatozoal apoptosis and testicular arsenic concentration. The subsequent results are presented here.

5.4.1 Effect of FHPD on testicular mRNA level expression of Bax and Bcl-2 in arsenic exposed state

Study was performed to explore the molecular mechanism involved in arsenic-induced apoptosis in testicular tissues and accordingly the mRNA levels of pro-apoptotic gene Bax and anti-apoptotic gene Bcl-2 were evaluated along with β-actin as reference gene. The PCR data revealed that the transcriptional expression of pro-apoptosis factor Bax was distinctly increased ($p<0.001$) in the testes of arsenic treated rats in comparison to that of control rats (Figure 13a). FHPD supplementation significantly decreased ($p<0.001$) the expression of Bax to near normal level (Figure 13a). Conversely the expression of Bcl-2, the anti-apoptosis factor was down-regulated ($p<0.001$) upon arsenic exposure in comparison to that of control (Figure 13b). Up-regulation ($p<0.001$) of Bcl-2 gene expression was seen in the FHPD supplemented group in spite of arsenic exposure (Figure 13b). The ratio of Bcl-2/Bax strikingly decreased ($p<0.001$) in arsenic exposed state indicating cellular susceptibility towards apoptosis (Figure 6c). The said ratio was seen to be increased significantly ($p<0.001$) in supplemented group demonstrating recovery from apoptosis (Figure 13c).

5.4.2 Role of FHPD on testicular protein level expression of Bax and Bcl-2 under arsenic insult

After analyzing the RT-qPCR data subsequently the study on the protein (Bax and Bcl-2) expression level was performed. Similar findings were noted as protein level of pro-apoptosis gene Bax was noticeably amplified ($p<0.001$) upon arsenic treatment in comparison to that of control group. Interestingly the protein level of anti-apoptosis gene Bcl-2 was markedly impaired ($p<0.001$) in arsenic treated group with respect to control group (Figure 14c). Up-regulation of Bax and down-regulation of Bcl-2 precisely specify the onset of arsenic mediated apoptosis in treated group (Figure 14b). FHPD supplementation fascinatingly decreased the Bax expression

($p<0.001$) to near normal level and also caused the increased Bcl-2 expression ($p<0.001$) to near control level (Figure 14c & b).

5.4.3 Effect of FHPD on testicular protein level expression of Caspase 9 and Caspase 3 under arsenic stress

The extent of apoptosis in testicular tissue was further evaluated by estimating the expression of caspase 9 and caspase 3 proteins. The immunoblot results illustrated the increased expression of procaspase-9 and cleaved caspase-9 and subsequently procaspase-3, cleaved caspase-3 ($p<0.001$ in all the cases) in arsenic intoxicated testicular tissues in comparison to the control values (Figure 15 b, c, e & f). In FHPD supplemented group their expressions were relatively lower ($p<0.001$ in all the cases) and maintained at in close proximity to control levels (Figure 15 b, c, e & f). These end results indicated that FHPD hindered the arsenic induced apoptosis in testicular tissues.

5.4.4 Effect of FHPD on spermatozoal apoptosis in arsenic intoxicated rats

Flow cytometry separated the population of spermatozoa into four groups: live cells, necrotic cells, early apoptotic cells and late apoptotic cells (Figure 16). Arsenic treatment caused increased incidence of early apoptotic cells ($p<0.001$), late apoptotic cells ($p<0.001$) and necrotic cells ($p<0.001$) (Table 16). Subsequently FHPD supplementation lowered their frequency ($p<0.001$, $p<0.001$ and $p<0.05$ respectively) even though notable difference still persisted with control group ($p<0.001$, $p<0.001$ and $p<0.001$ respectively) (Table 16).

5.4.5 Role of FHPD on arsenic deposition in testicular tissues in arsenic exposed rats

Quantification of arsenic deposition in testicular tissues was carried out by the help of atomic absorption spectroscopy. In treated group the level of arsenic deposition was significantly high ($p<0.001$) compared to that of control group (Figure 17). Nevertheless FHPD supplementation resulted maintenance of tissue arsenic level near normal (Figure 17).

6. Discussion

The present study was designed to investigate the protective role of FHPD supplementation on adult male rats against the toxic effect of arsenic on structure-function alterations on male reproductive end points involving testes and spermatozoa. Another major purpose of this study was to explore whether the FHPD supplementation can mitigate the arsenic mediated apoptosis on testicular germ cell and spermatozoa.

Arsenic at a dose of 3mg/kg/day given for a period of 30 days didn't cause any significant change on the body weight, food and water intake indicating no overt general toxicity. But arsenic exposed rats exhibited aggressive behavioral pattern and loss of hair. Arsenic significantly reduced the weight of testis, epididymis, seminal vesicle and prostate gland which were in agreement with the earlier report [73]. As evidenced from testicular histology and ultrastructural study, arsenic caused severe damage of seminiferous tubules and interstitium along with desquamation of epithelial cells, development of vacuoles, disorientation of seminiferous germinal epithelium, lesser spermatozoal concentration in the lumen and germ cell necrosis. These findings are in agreement with Bashir N et al. [74]. Morphometric alterations were probably the consequences which aroused due to decrease in the total volume of testis [75, 76]. Leydig cells and Sertoli cells are the two edged sword responsible for maintenance of structural integrity and functional facet of seminiferous tubules. Arsenic treatment reduced their numbers which might be due to accumulated ROS [23, 77–79]. Decline in Leydig cells led to constrained production of testosterone and Sertoli cell damages restricted nutrition to different spermatogonial cells/germ cells. Arsenic mediated oxidative stress might be the primary reason behind such histological alterations [80]. FHPD can mitigate such structural alterations primarily by scavenging ROS and secondarily by retaining the normal functioning of Leydig and Sertoli Cell.

Arsenic threat altered normal spermatozoa potentials to a greater extent which partly may be due to its adverse effect on spermatogenesis and also due to the altered environment in the epididymis. As arsenic is known to be a thiol inhibiting substance [78] and its presence in the epididymis may be the key reason for the decrease in motility and viability due to oxidation of various proteins. The reason behind reduction in HOS+ve spermatozoa may be due to the peroxidation of polyunsaturated fatty acids in the sperm plasma membranes caused by arsenic

generated free radicals [81]. Spermatozoal structural anomalies occurred due to morphological alterations during spermatogenic growth are classified into primary and secondary abnormalities according to [82]. Rudimentary tail was the only primary abnormality caused due to eccentricity in the process of spermatogenesis whereas bent mid-piece, curved mid-piece, bent tail, curved tail, headless tail, curved tail and coiled tail were considered as the secondary abnormalities caused by fundamental problem with the process of maturation in epididymis [83]. Here, the increased secondary abnormalities again pose a serious issue regarding the role of epididymis in it. Impairment of acrosome development occurs as Sertoli cell-germ cell interactions get hampered due to testosterone deficiency [16]. These might be the reason behind the acute dorsoventrally constrictions in the mid-region of spermatozoa (head) with swelled sub acrosomal material in arsenic treated rats. Post nuclear cap is responsible for maintenance of structural stability of sperm head and it got distorted with many serrations under arsenic threat that eventually resulted in inhomogeneous plasma membrane of sperm head. The exact reason behind shortening in the length of post acrosomal dense laminar region under arsenic insult is still not clear. However FHPD supplementation prior to arsenic treatment maintained the spermatozoa structure and potentials more or less similar to that of control group.

Arsenic exposure was also found to affect the growth and differentiation of germ cells as well as the degeneration at different levels of their maturation particularly at the level of spermatogonia, primary spermatocytes and spermatid compared to those of control group. The ratio of mPSc to 7Sd denotes 1:4 theoretically and any divergence in this ratio indicates impairment of spermatogenic process as testified by Clermont Y [46]. Optimal level of testosterone is crucial for completion of meiosis, formation of spermatids and conversion of pachytene spermatocytes to round spermatids [84]. Reduction of testosterone level under the influence of arsenic as observed in this study which attests the earlier report [14] from this laboratory might be the possible reason for interruption of growth and differentiation of germ cell as well as their degeneration culminating to deterioration of testicular architecture [85, 86]. In this study, arsenic trioxide caused marked decrease in the activities of Δ5 3β-HSD and 17β-HSD which might be responsible for the reduced synthesis of testosterone and these findings are in harmony with earlier reports [14, 28]. Arsenic has also been reported to effect the gene expression of these key regulatory steroidogenic enzymes [17]. Spermatogenesis is strongly associated with activities of several enzymes in spermatogenic cells. LDH, ACP, ALP and γ-GT

are important enzymatic biomarkers of testes involved in metabolism, germinal epithelium proliferation and differentiation, transportation of nutrients from sertoli cells to various germ cells [74]. Increased LDH activity indicates impaired energy metabolism and deformity in spermatogenic cell [11]. A recent study states that decrease in γ-GT activity is suggestive of impaired Sertoli cell function and spermatogenesis, manifested by gross testicular atrophy, poor histoarchitecture of the testis, cessation of spermatogenesis, and germ cell maturation arrest [87]. The enhanced activities of ALP and ACP might reflect the release of these non-specific phosphatases from the lysosomes of the degenerating cells and rapid catabolism of the testicular cells [88]. FHPD restores the activities of these enzymes by reducing ROS mediated lipid peroxidation and thus facilitate spermatogenic development and maintenance of spermatogenesis. FHPD maintained normal steroidogenesis by sustaining the enzymatic activities of Δ5 3β-HSD and 17β-HSD which in turn enhances testosterone production [89]. So this might be the potential reason behind FHPD mediated protection of testicular spermatogenesis, histoarchitecture of testes and spermatozoa. Another explanation is FHPD preserved sertoli cell number which in turn shielded germ cell maturation and differentiation.

The other noteworthy feature of arsenic toxicity is an exacerbated testicular oxidative stress that has been known to compromise both spermatozoal production and steroid hormone synthesis, and threats male reproduction [90]. The present findings demonstrate that arsenic challenged the testicular set up to breach the control over the free radical production and antioxidant defense system, precipitating a state of testicular oxidative stress. Increased production of MDA and PC content in arsenic-treated testis as match up to the FHPD-supplemented group, therefore, argues that arsenic provokes ROS generation. Arsenic also altered the activity of the antioxidant enzymes and liberated radical foragers to make matters worse. The attenuated testicular activities of SOD, catalase, GPx, GR, GST and decreased GSH content in the arsenic-treated group, in contrast to those of the control and FHPD-fed groups, therefore, reinforce the proposition that arsenic not only provokes the production of free radicals but disrupts the detoxification mechanisms as well. Similar scenario was also observed in cauda epididymis. Electron leakage from sperm mitochondria constitutes the primary source of ROS in them [91]. However, unlike most somatic cells, these cells are moderately insufficient in ROS-rummaging catalysts because of the constrained volume and confined conveyance of cytosolic space. As a consequence, when arsenic induced ROS by the sperm mitochondria is in abundance,

at that point the gamete's constrained endogenous antioxidant protections are quickly overpowered following oxidative harm. Spermatozoa, therefore, mainly depend on the antioxidant defense obtainable by the testis and epididymis. FHPD supplementation, by contrast, could significantly avert the generation of ROS and sustain the antioxidant system to manage the redox homeostasis and arsenic-induced crisis efficiently in testes, cauda epididymis and as well as in spermatozoa.

Arsenic was also responsible for the apparent changes in the histoarchitecture of cauda epididymis which include, decrease in number of stereocilia in the inner wall lining and also thinning of pseudo-stratified columnar epithelium. Likewise FHPD protected from over production of ROS as a result the caudal histoarchitecture was restored. Arsenic induced ROS unswervingly results in DNA oxidation which ultimately leads to DNA fragmentation. In this study, the DNA isolated from testicular and cauda epididymal tissues of arsenic-treated rats showed degradation into oligonucleotide fragments forming a clear ladder pattern when analyzed by gel electrophoresis. Fragmented DNA may eventually be either repaired or it may pursue towards apoptosis. Structural integrity of spermatozoa is associated with its maturity and also dependent on the quality of spermatozoal DNA. Aniline blue selectively stains lysine-rich histones and has been used for the purpose of those sperm chromatin condensation anomalies that are related to residual histones [92]. In agreement with the results of a previous study [93], we also found a high percentage of AB-positive sperm i.e. sperm with incomplete or defective DNA condensation in arsenic treated rats. This suggests arsenic exposure led to negative effect on chromatin condensation of the sperm which leads to formation of immature sperm. The loss of DNA integrity by arsenic was again established by A/O staining method where DNA denaturation is evaluated via meta-chromatic shifting of AO fluorescence from green (native double-stranded DNA) to red (denatured single-stranded DNA) [92]. The present data showed a significant increase in spermatozoa with red fluorescence from arsenic treated group when compared with control group which is in agreement with findings of Talebi AR [94]. This means that there is more DNA damage in sperms of arsenic intoxicated rats. Secondly, by sperm comet assay analysis where the genotoxic effect of arsenic was evident by an increase in the comet parameters like % tail DNA, tail movement, olive tail movement and decrease in % head DNA. Nava-Hernandez et al. [95] reported that toxic metals (lead, cadmium and arsenic) caused DNA damage in primary spermatocytes of rats with chronic exposure. In addition, Khan et al. [28]

showed that arsenic increased the DNA damage index in the spermatozoa of rats. FHPD drastically reduced ROS generation which in turn protected testes, cauda epididymis and also spermatozoa from DNA damage.

Apoptosis is a complex event regulated by a well tuned balance of inducer and repressor factors, such as the Bcl-2 family. Both Bcl-2 and Bax belong to the Bcl-2 family, but they have adverse functions in the apoptosis process. It has been proved that an increase in the ratio of Bax/Bcl-2 in tissues could predispose tissues to apoptotic stimuli [96]. In this study the mRNA level expression of Bax was increased and Bcl-2 was decreased in testes of arsenic treated rats. These findings suggested that the co-opponent effect of Bax and Bcl-2 might be responsible for the modulation of arsenic-induced apoptosis in rat testis as the ratio of Bcl-2 to Bax decrease upon arsenic treatment. Moreover, Bax can promote apoptosis by homodimerization or hetrodimerization of Bcl-2 [97]. In this study, the immune reactivity of Bax protein was expressed principally higher, while Bcl-2 protein was lesser expressed in testes of arsenic-treated rats. Increased expression of Bax following decreased expression of Bcl-2 in the arsenic-treated testes and attenuated expression of Bax along with increased Bcl-2 expression next to FHPD diet suggest that arsenic initiates testicular apoptosis involving the mitochondria-mediated pathway while FHPD forbids this detrimental exploit. Activation of Bax protein leads to the formation of pores in the mitochondria and results in the collapse of the electrochemical gradient across the mitochondrial membrane, then cytochrome c is released into cytoplasm where it is associated with procaspase-9/Apaf-1. This complex in turn activates a downstream caspase program, leading ultimately to apoptotic cell death [98]. The role of caspase-3 as the effector molecule in the death cascade of the apoptotic pathway is well established [99]. It plays a central role in the execution pathway of apoptosis and is a final caspase that gets activated irrespective of whether the path was initiated by the extrinsic or intrinsic mechanisms. Caspase-3 is activated by the upstream caspase- 8 and caspase-9, and since it serves as a convergence point for different signalling pathways, it is considered as a readout in an apoptosis assay. The results have indicated increased expression of procaspase-9, especially cleaved caspase-9 in the arsenic-treated testes that validated the release of cytochrome c into cytoplasm and initiation of downstream caspase cascade. Finally increased expression of procaspase-3 and cleaved caspase-3 in the testicular tissue that onsets of apoptosis-mediated protease activation and cell death. The attenuated expression of both procaspase-9 and 3 along with caspase-9 and 3 in the FHPD-

supplemented group clearly reflects an overall hindrance of the arsenic-mediated apoptosis. As we report here, increase in caspase-9/3 activity and alteration in the ratio of Bcl-2/Bax could be a key determining factor in the release of cytochrome c, the activation of caspase-9/3 and the initiation of apoptosis. A decrease in this ratio may exacerbate apoptosis, and increasing this ratio may reverse the deleterious effect of cytotoxic stimuli [97, 100]. While Bax has been shown to trigger cell death, the anti-apoptotic Bcl-2 can block cytochrome c release and caspase activation [100, 101]. Similar observation was also found in spermatozoa after screening of apoptosis by Annexin V and Pi, however FHPD lowered their percentage significantly. Arsenic deposition in testes was seen to be diminished after FHPD supplementation as FHPD facilitates biomethylation of arsenic which in turn excretes arsenic through urine [40].

FHPD comprising of a combination of casein and pea have been found to be an effective management strategy to combat arsenic mediated testicular and spermatozoal anomalies. Pea and casein are known to have anti-oxidant properties and facilitates arsenic biomethylation. Casein and casein-derived peptides were able to inhibit enzymatic and non-enzymatic lipid peroxidation, suggesting they were preferred targets for the free radical intermediates [102]. The antioxidant feature was not lost with the dephosphorylation or proteolysis of the proteins [102]. Proteins and peptides together with the fatty acid, be the target of oxidative degradations and either initiate further unwanted radical – mediated side reactions or terminate chain reactions depending on the ability of the resulting proton/ peptide radical [102]. The proteins owe their antioxidant activity to their constituent amino acids. The antioxidant activities of aromatic amino acids such as tyrosine, phenylalanine and tryptophan and the sulfur-containing amino acid, cysteine, are due to their ability to donate protons to free radicals [103].

7. Conclusion

Therefore, the study concluded that casein–pea-enriched protein diet /FHPD was successful in mitigating the toxic effects of arsenic on male reproductive system of adult rats. Furthermore, FHPD was able to manage the ROS mediated testicular DNA damage and subsequent apoptosis. These findings inferred that the diet successfully attenuated several deleterious effects of arsenic on epididymal spermatozoal population.

8. Significance of this study

Measures to combat arsenic pollution of ground water are inadequate in the rural sectors. This study significantly countered arsenic induced reproductive toxicity upon supplementation of formulated high protein diet comprising of pea and milk protein. Enhanced arsenic biomethylation leads to faster excretion of arsenic, thus preventing DNA hypomethylation, a trigger for arsenic-induced apoptosis. The beneficial inputs of this dietary regime include the high methionine content of pea and strong antioxidative nature of both pea and casein. Nutrition Research will be benefited from the positive results of our work. This work has the potential to guide future government policies towards arsenic toxicity management.

9. Acknowledgement

Scanning electron microscopy and FACS was performed at Centre for Research in the Nanoscience and Nanotechnology, University of Calcutta. Atomic absorption spectroscopy was performed at School of Environmental Studies, Jadavpur University.

10. Abbreviations

AB: Aniline blue

ACP: Acid phosphatase

ALP: Alkaline phosphatase

AO: Acridine orange

CAT: Catalase

FACS: Fluorescent activated cell sorter

FHPD: Formulated high protein diet

DCFDA: 2,7-dichlorofluorescin

DNPH: 2,4-dinitrophenylhydrazine

ELISA: Enzyme linked immunosorbent assay

γ-GT: Gamma glutamyl transferase

GPx: Glutathione peroxidase

GR: Glutathione reductase

GSH: Glutathione

GST: Glutathione S-transferase

H/E: Hematoxylin-eosin staining

HOST: Hypo-osmotic swelling test

HSD: Hydroxysteroid dehydrogenase

HSD: Highest significant difference

LDH: Lactate dehydrogenase

LPO: Lipid peroxidation

LSD: Least significant difference

MDA: Malondialdehyde

NMS: Non-motile sperm

NPMS: Non-progressively motile sperm

PC: Protein carbonyl

PMS: Progressively motile sperm

ROS: Reactive oxygen species

SOD: Superoxide dismutase

SEM: Scanning electron microscopy

11. References

[1] WHO (ed). *Guidelines for drinking-water quality*. 4th ed. WHO, 2011.

[2] Kumar, Rahman MS, Iqubal MA, et al. Ground water arsenic contamination: A local survey in India. *Int J Prev Med* 2016; 7: 100.

[3] Ratnaike RN. Acute and chronic arsenic toxicity. *Postgr Med J* 2003; 79: 391–396.

[4] Mazumder, Ghosh A, Majumdar KK, et al. Arsenic contamination of ground water and its health impact on population of district of Nadia, West Bengal, India. *Indian J Community Med* 2010; 35: 331.

[5] Wares MA, Awal MA, Das SK, et al. Chronic natural arsenic exposure affecting histoarchitecture of gonads in Black Bengal goats (Capra aegagrushircus). *J Adv Vet Anim Res* 2015; 2: 128–133.

[6] Lima G, Sertorio M, Souza A, et al. Fertility in male rats: Disentangling adverse effects of arsenic compounds. *Reprod Toxicol* 2018; 78: 130–140.

[7] Wang A, Holladay S, Wolf D, et al. Reproductive and developmental toxicity of arsenic in rodents: a review. *Int J Toxicol* 2006; 25: 319–331.

[8] Apostoli P, Catalani S. Metal ions affecting reproduction and development. *Met Ions Life Sci* 2011; 8: 263–303.

[9] Balabanic D, Rupnik M, Klemencic AK. Negative impact of endocrine-disrupting compounds on human reproductive health. *Reprod Fertil Dev* 2011; 23: 403–416.

[10] Sengupta M, Deb I, Sharma G, et al. Human sperm and other seminal constituents in male infertile patients from arsenic and cadmium rich areas of Southern Assam. *Syst Biol Reprod Med* 2013; 59: 199–209.

[11] Jana K, Jana S, Samanta PK. Effects of chronic exposure to sodium arsenite on hypothalamo-pituitary-testicular activities in adult rats: Possible an estrogenic mode of action. *Reprod Biol Endocrinol*; 4. Epub ahead of print February 2006. DOI: 10.1186/1477-7827-4-9.

[12] Sarkar M, Chaudhuri GR, Chattopadhyay A, et al. Effect of sodium arsenite on spermatogenesis, plasma gonadotrophins and testosterone in rats. *Asian J Androl* 2003; 5: 27–31.

[13] Momeni HR, Oryan S, Eskandari N. Effect of vitamin E on sperm number and testis histopathology of sodium arsenite-treated rats. *Reprod Biol* 2012; 12: 171–181.

[14] Mukhopadhyay PK, Dey A, Mukherjee S, et al. The effect of coadministration of alpha-tocopherol and ascorbic acid on arsenic trioxide-induced testicular toxicity in adult rats. *J Basic Clin Physiol Pharmacol* 2013; 24: 245–253.

[15] Pant N, Murthy RC, Srivastava SP. Male reproductive toxicity of sodium arsenite in mice. *Hum Exp Toxicol* 2004; 23: 399–403.

[16] Ferreira M, Matos RC, Oliveira H, et al. Impairment of mice spermatogenesis by sodium arsenite. *Hum Exp Toxicol* 2012; 31: 290–302.

[17] Chiou TJ, Chu ST, Tzeng WF, et al. Arsenic trioxide impairs spermatogenesis via reducing gene expression levels in testosterone synthesis pathway. *Chem Res Toxicol* 2008; 21: 1562–1569.
[18] Santra A, Maiti A, Das S, et al. Hepatic damage caused by chronic arsenic toxicity in experimental animals. *J Toxicol Clin Toxicol* 2000; 38: 395–405.
[19] Ramanathan K, Shila S, Kumaran S, et al. Protective role of ascorbic acid and alpha-tocopherol on arsenic-induced microsomal dysfunctions. *Hum Exp Toxicol* 2003; 22: 129–136.
[20] Liu S, Athar M, Lippai I, et al. Induction of oxyradicals by arsenic: implication for mechanism of genotoxicity. *Proc Natl Acad Sci U S A* 2001; 98: 1643–1648.
[21] Nandi D, Patra RC, Swarup D. Effect of cysteine, methionine, ascorbic acid and thiamine on arsenic-induced oxidative stress and biochemical alterations in rats. *Toxicology* 2005; 211: 26–35.
[22] Flora SJ. Arsenic-induced oxidative stress and its reversibility. *Free Radic Biol Med* 2011; 51: 257–281.
[23] Chang SI, Jin B, Youn P, et al. Arsenic-induced toxicity and the protective role of ascorbic acid in mouse testis. *Toxicol Appl Pharmacol* 2007; 218: 196–203.
[24] Uslu R, Sanli UA, Sezgin C, et al. Arsenic trioxide-mediated cytotoxicity and apoptosis in prostate and ovarian carcinoma cell lines. *Clin Cancer Res* 2000; 6: 4957–4964.
[25] Selvaraj V, Armistead MY, Cohenford M, et al. Arsenic trioxide (As(2)O(3)) induces apoptosis and necrosis mediated cell death through mitochondrial membrane potential damage and elevated production of reactive oxygen species in PLHC-1 fish cell line. *Chemosphere* 2013; 90: 1201–1209.
[26] Zheng Y, Yamaguchi H, Tian C, et al. Arsenic trioxide (As(2)O(3)) induces apoptosis through activation of Bax in hematopoietic cells. *Oncogene* 2005; 24: 3339–3347.
[27] Salakou S, Kardamakis D, Tsamandas A, et al. Increased Bax/Bcl-2 Ratio Up-regulates Caspase-3 and Increases Apoptosis in the Thymus of Patients with Myasthenia Gravis. *In Vivo (Brooklyn)*; 21.
[28] Khan SA, Telang A, Malik J. Arsenic-induced oxidative stress , apoptosis and alterations in testicular steroidogenesis and spermatogenesis in wistar rats : ameliorative effect of curcumin.
[29] Modi M, Mittal M, Flora SJS. Combined administration of selenium and meso-2,3-dimercaptosuccinic acid on arsenic mobilization and tissue oxidative stress in chronic arsenic-exposed male rats. *Indian J Pharmacol* 2007; 39: 107–114.
[30] Ramanathan K, Balakumar BS, Panneerselvam C. Effects of ascorbic acid and alpha-tocopherol on arsenic-induced oxidative stress. *Hum Exp Toxicol* 2002; 21: 675–680.
[31] Modi M, Kaul RK, Kannan GM, et al. Co-administration of zinc and n-acetylcysteine prevents arsenic-induced tissue oxidative stress in male rats. *J Trace Elem Med Biol* 2006; 20: 197–204.
[32] Brinkel J, Khan MH, Kraemer A. A Systematic Review of Arsenic Exposure and Its Social and Mental Health Effects with Special Reference to Bangladesh. *Int J Environ Res Public Health* 2009; 6: 1609.
[33] Mukherjee S, Mukhopadhyay PK. Studies on arsenic toxicity in male rat gonads and its protection by high dietary protein supplementation. *Al Ameen J Med Sci* 2009; 2: 73–77.
[34] Mondal S, Mukherjee S, Chaudhuri K, et al. Prevention of arsenic-mediated reproductive toxicity in adult female rats by high protein diet. *Pharm Biol*,

http://www.ncbi.nlm.nih.gov/entrez/query.fcgi?cmd=Retrieve&db=PubMed&dopt=Citation&list_uids=23859609 (2013).
[35] Bansal AK, Mehta J, Mehta M, et al. In vitro effect of soybean (Glycine max L. Merr) lectin on lipid peroxidation in pyridoxine deficient albino rats. *Indian J Exp Biol* 1987; 25: 800–801.
[36] Maiti S, Chatterjee A. Effects on levels of glutathione and some related enzymes in tissues after an acute arsenic exposure in rats and their relationship to dietary protein deficiency. *Arch Toxicol* 2001; 75: 531–537.
[37] Mukherjee S Darbar D, Mitra, C DD. Dietary intervention affects arsenic generated nitric oxide and reactive intermediate toxicity in islet cell of rats. *Curr Sci* 2003; 85: 93–786.
[38] Wong P, Kitts D. A comparison of the buttermilk solids functional properties to nonfat dried milk, soy protein isolate, dried egg white, and egg yolk powders. *J Dairy Sci* 2003; 86: 746–754.
[39] Joshi JG, Handler P. Biosynthesis of Trigonelline*. *J Biol Chem* 1960; 235: 2981–2983.
[40] Pimparkar BD, Bhave A. Arsenicosis: review of recent advances. *J Assoc Physicians India* 2010; 58: 617-624,629.
[41] Buchet J, Lauwerys R. Study of factors influencing the in vivo methylation of inorganic arsenic in rats. *Toxicol Appl Pharmacol* 1987; 91: 65–74.
[42] Lammon C, Hood R. Effects of protein deficient diets on the developmental toxicity of inorganic arsenic in mice. *Birth Defects Res B Dev Reprod Toxicol* 2004; 71: 124–134.
[43] Biswas P, Mukhopadhyay A, Kabir SN, et al. High-Protein Diet Ameliorates Arsenic-Induced Oxidative Stress and Antagonizes Uterine Apoptosis in Rats. *Biol Trace Elem Res*; 192. Epub ahead of print 2019. DOI: 10.1007/s12011-019-1657-2.
[44] AM J. *Male Infertility. A guide for clinician*. London UK: Blackwell Science Ltd, 2000.
[45] Romero D, Officinalis R, En Ratas L), et al. An Electron Microscopic Study of the Antifertility Potential of Rosemary (Rosmarinus officinalis L.) in Male Albino Rats. *Int J Morphol* 2012; 30: 666–672.
[46] Leblond CP, Clermont Y. Definition of the stages of the cycle of the seminiferous epithelium in the rat. *Ann N Y Acad Sci* 1952; 55: 548–573.
[47] Abercrombie M. Estimation of nuclear population from microtome sections. *Anat Rec*; 94. Epub ahead of print 1946. DOI: 10.1002/ar.1090940210.
[48] WHO. *WHO Laboratory Manual for the Examination of Human Semen and Semen–Cervical Mucus Interaction* . 4th ed. Cambridge: UK: Cambridge University Press, 1999.
[49] Jeyendran RS, Van der Ven HH, Zaneveld LJ. The hypoosmotic swelling test: an update. *Arch Androl* 1992; 29: 105–116.
[50] Aladakatti RH, Ahamed RN. Ultrastructural changes in Leydig cells and cauda epididymal spermatozoa induced by Azadirachta indica leaves in albino rats. *Phyther Res* 2005; 19: 756–766.
[51] Talaly P. Hydroxysteroid dehydrogenases. In: R.B. C (ed) *Methods in enzymology*. New York: Academic Press, 1962, pp. 512–516.
[52] Jarabak GA. *Soluble 17b-hydroxisteroid dehydrogenase on human placenta*. New York: Academic Press, 1969.
[53] Vanha-Perttula T, Nikkanen V. Acid phosphatases of the rat testis in experimental conditions. *Acta Endocrinol (Copenh)* 1973; 72: 376–390.
[54] Malymy M, Horecker B. Alkaline phosphatase. In: *In Methods in Enzymology* . New York: Academic Press, 1996, pp. 639–642.

[55] Ohkawa H, Ohishi N, Yagi K. Assay for lipid peroxides in animal tissues by thiobarbituric acid reaction. *Anal Biochem* 1979; 95: 351–358.
[56] Levine RL, Williams JA, Stadtman EP, et al. Carbonyl assays for determination of oxidatively modified proteins. *Methods Enzymol* 1994; 233: 346–357.
[57] Zakowski JJ, Tappel AL. A semiautomated system for measurement of glutathione in the assay of glutathione peroxidase. *Anal Biochem* 1978; 89: 430–436.
[58] Martin JP, Dailey M, Sugarman E. Negative and positive assays of superoxide dismutase based on hematoxylin autoxidation. *Arch Biochem Biophys* 1987; 255: 329–336.
[59] Beers Jr. RF, Sizer IW. A spectrophotometric method for measuring the breakdown of hydrogen peroxide by catalase. *J Biol Chem* 1952; 195: 133–140.
[60] Boyland E, Chasseaud LF. The role of glutathione and glutathione S-transferases in mercapturic acid biosynthesis. *Advances in enzymology and related areas of molecular biology* 1969; 32: 173–219.
[61] Flohe L, Gunzler WA. Assays of glutathione peroxidase. *Methods Enzym* 1984; 105: 114–121.
[62] Smith IK, Vierheller TL, Thorne CA. Assay of glutathione reductase in crude tissue homogenates using 5,5'-dithiobis(2-nitrobenzoic acid). *Anal Biochem* 1988; 175: 408–413.
[63] Wyllie AH, Kerr JFR, Currie AR. Cell Death: The Significance of Apoptosis. *Int Rev Cytol* 1980; 68: 251–306.
[64] Compton M. A biochemical hallmark of apoptosis: internucleosomal degradation of the genome. *Cancer Metastasis Rev* 1992; 11: 105–119.
[65] Terquem A, Dadoune JP. Aniline Blue Staining of Human Spermatozoon Chromatin. Evaluation of Nuclear Maturation. *Sperm Cell* 1983; 249–252.
[66] Tejada R, Mitchell J, Norman A, et al. A test for the practical evaluation of male fertility by acridine orange (AO) fluorescence. *Fertil Steril* 1984; 42: 87–91.
[67] Trivedi P, Kushwaha S, Tripathi D, et al. Evaluation of male germ cell toxicity in rats: correlation between sperm head morphology and sperm comet assay. *Mutat Res* 2010; 703: 115–121.
[68] Anzar M, He L, Buhr M, et al. Sperm Apoptosis in Fresh and Cryopreserved Bull Semen Detected by Flow Cytometry and Its Relationship with Fertility. *Biol Reprod* 2002; 66: 354–360.
[69] Hossain M, Johannisson A, Wallgren M, et al. Flow cytometry for the assessment of animal sperm integrity and functionality: state of the art. *Asian J Androl* 2011; 13: 406–419.
[70] Mahdavi S, Khodarahmi P, Roodbari N. Effects of cadmium on Bcl-2/ Bax expression ratio in rat cortex brain and hippocampus. *Hum Exp Toxicol* 2018; 37: 321–328.
[71] Rupnow H, Phernetton T, Shaw C, et al. Endothelial vasodilator production by uterine and systemic arteries. VII. Estrogen and progesterone effects on eNOS. *Am J Physiol Heart Circ Physiol*; 280. Epub ahead of print 2001. DOI: 10.1152/AJPHEART.2001.280.4.H1699.
[72] Chowdhury N, Das A, Joardar M, et al. Flow of arsenic between rice grain and water: Its interaction, accumulation and distribution in different fractions of cooked rice. *Sci Total Environ*; 731. Epub ahead of print 20 August 2020. DOI: 10.1016/J.SCITOTENV.2020.138937.
[73] Prathima P, Pavani R, Sukeerthi S, et al. α-Lipoic acid inhibits testicular and epididymal

oxidative damage and improves fertility efficacy in arsenic-intoxicated rats. *J Biochem Mol Toxicol*; 32. Epub ahead of print 1 February 2018. DOI: 10.1002/jbt.22016.
[74] Bashir N, Shagirtha K, Manoharan V, et al. The molecular and biochemical insight view of grape seed proanthocyanidins in ameliorating cadmium-induced testes-toxicity in rat model: implication of PI3K/Akt/Nrf-2 signaling. *Biosci Rep* 2019; 39: 20180515.
[75] Jahan S, Iftikhar N, Ullah H, et al. Alleviative effect of quercetin on rat testis against arsenic: a histological and biochemical study. *Syst Biol Reprod Med* 2015; 61: 89–95.
[76] Mehrzadi S, Bahrami N, Mehrabani M, et al. Ellagic acid: A promising protective remedy against testicular toxicity induced by arsenic. *Biomed Pharmacother* 2018; 103: 1464–1472.
[77] Sarkar S, Hazra J, Upadhyay S, et al. Arsenic induced toxicity on testicular tissue of mice. *Indian J Physiol Pharmacol* 2008; 52: 84–90.
[78] Manna P, Sinha M, Sil PC. Protection of arsenic-induced testicular oxidative stress by arjunolic acid. *Redox Rep* 2008; 13: 67–77.
[79] Mittal M, Flora SJ. Vitamin E supplementation protects oxidative stress during arsenic and fluoride antagonism in male mice. *Drug Chem Toxicol* 2007; 30: 263–281.
[80] Souza A, Marchesi S, Lima G, et al. Effects of Sodium Arsenite and Arsenate in Testicular Histomorphometry and Antioxidants Enzymes Activities in Rats. *Biol Trace Elem Res* 2016; 171: 354–362.
[81] Das J, Ghosh J, Manna P, et al. Taurine protects rat testes against NaAsO2-induced oxidative stress and apoptosis via mitochondrial dependent and independent pathways. *Toxicol Lett* 2009; 187: 201–210.
[82] Noakes D, Parkinson T, England G, et al. Arthur's Veterinary Reproduction and Obstetrics Eighth Edition. *J Chem Inf Model* 2001; 53: 1689–1699.
[83] Saba A, Oridupa O, Oyeyemi M, et al. Spermatozoa morphology and characteristics of male wistar rats administered with ethanolic extract of *Lagenaria Breviflora* Roberts. *African J Biotechnol* 2010; 8: 1170–1175.
[84] Chandra A, Ghosh R, Chatterjee A, et al. Amelioration of vanadium-induced testicular toxicity and adrenocortical hyperactivity by vitamin E acetate in rats. *Mol Cell Biochem* 2007; 306: 189–200.
[85] Reddy PS, Rani GP, Sainath SB, et al. Protective effects of N-acetylcysteine against arsenic-induced oxidative stress and reprotoxicity in male mice. *J Trace Elem Med Biol* 2011; 25: 247–253.
[86] Baltaci B, Uygur R, Caglar V, et al. Protective effects of quercetin against arsenic-induced testicular damage in rats. *Andrologia* 2016; 48: 1202–1213.
[87] Akhigbe R, Ajayi A. Testicular toxicity following chronic codeine administration is via oxidative DNA damage and up-regulation of NO and caspase 3. *bioRxiv* 2019; 796110.
[88] Abarikwu SO, Otuechere CA, Ekor M, et al. Rutin Ameliorates Cyclophosphamide-induced Reproductive Toxicity in Male Rats. *Toxicol Int* 2018; 19: 207–214.
[89] Biswas S, Kumar Mukhopadhyay P. Casein- and pea-enriched high-protein diet can take care of the reprotoxic effects of arsenic in male rats. *Andrologia*; 52. Epub ahead of print 1 June 2020. DOI: 10.1111/and.13560.
[90] Aitken RJ, Nixon B, Lin M, et al. Proteomic changes in mammalian spermatozoa during epididymal maturation. *Asian Journal of Andrology* 2007; 9: 554–564.
[91] Koppers A, Mitchell L, Wang P, et al. Phosphoinositide 3-kinase signalling pathway involvement in a truncated apoptotic cascade associated with motility loss and oxidative

DNA damage in human spermatozoa. *Biochem J* 2011; 436: 687–698.
[92] Pourmasumi S, Khoradmehr A, Rahiminia T, et al. Evaluation of Sperm Chromatin Integrity Using Aniline Blue and Toluidine Blue Staining in Infertile and Normozoospermic Men. *J Reprod Infertil* 2019; 20: 95.
[93] Shittu SA, Shittu S-T, Akindele OO, et al. Protective action of N-acetylcysteine on sperm quality incyclophosphamide-induced testicular toxicity in male Wistar rats. *JBRA Assist Reprod* 2019; 23: 83.
[94] Talebi A, Khorsandi L, Moridian M. The effect of zinc oxide nanoparticles on mouse spermatogenesis. *J Assist Reprod Genet* 2013; 30: 1203–1209.
[95] Nava-Hernández M, Hauad-Marroquín L, Bassol-Mayagoitia S, et al. Lead-, cadmium-, and arsenic-induced DNA damage in rat germinal cells. *DNA Cell Biol* 2009; 28: 241–248.
[96] Perlman H, Zhang X, Chen MW, et al. An elevated bax/bcl-2 ratio corresponds with the onset of prostate epithelial cell apoptosis. *Cell Death Differ 1999 61* 1999; 6: 48–54.
[97] Eleawa S, Alkhateeb M, Alhashem F, et al. Resveratrol reverses cadmium chloride-induced testicular damage and subfertility by downregulating p53 and Bax and upregulating gonadotropins and Bcl-2 gene expression. *J Reprod Dev* 2014; 60: 115–127.
[98] Kuwana T, Newmeyer D. Bcl-2-family proteins and the role of mitochondria in apoptosis. *Curr Opin Cell Biol* 2003; 15: 691–699.
[99] Danial N, Korsmeyer S. Cell death: critical control points. *Cell* 2004; 116: 205–219.
[100] Yiran Z, Chenyang J, Jiajing W, et al. Oxidative stress and mitogen-activated protein kinase pathways involved in cadmium-induced BRL 3A cell apoptosis. *Oxid Med Cell Longev*; 2013. Epub ahead of print 2013. DOI: 10.1155/2013/516051.
[101] Xu J, Lian L, Wu C, et al. Lead induces oxidative stress, DNA damage and alteration of p53, Bax and Bcl-2 expressions in mice. *Food Chem Toxicol* 2008; 46: 1488–1494.
[102] Sandrine G, Carmen G, Wichers H. Caseins and Casein Hydrolysates. 2. Antioxidative Properties and Relevance to Lipoxygenase Inhibition. *J Agric Food Chem* 2000; 49: 295–302.
[103] Rajapakse N, Mendis E, Jung W-K, et al. Purification of a radical scavenging peptide from fermented mussel sauce and its antioxidant properties. *Food Res Int* 2005; 2: 175–182.

Figures and Tables

Table 1 Composition of normal diet and formulated high protein diet (FHPD) per 100 gm

Components	Composition	Normal diet (gm %)	FHPD (gm %)
Proteins	Whole wheat flour	3.62	-
	Roasted Bengal gram flour	4.38	-
	Casein	10	25
	Pea	-	7
	Total	18	32
Carbohydrates		71	57
Lipids		7	7
Minerals and vitamins		4	4
Energy		4.178 kcal/g	4.180 kcal/g

Table 2 Primer sequences used for real-time PCR

Primer Sequence (5'-3')			
Target Gene	Forward	Reverse	Size (bp)
Bax	AACATGGAGCTGCAGAGGAT	CCAGTTGAAGTTGCCGTCTG	105
BCl-2	GTGGACAACATCGTCCTGTG	GAGCAGCGTCTTCAGAGACA	156
β-actin	CGCGAGTACAACCTTCTTGC	CGTCATCCATGGCGAACTGG	70

PCR- polymerase chain reaction

Table 3 Effect of FHPD supplementation on body weight, organ weight and gravimetric index of arsenic treated adult rats

Parameters		Control (Gr – I)	Treated (Gr - II)	Supplement (Gr – III)
Difference in b wt (F-I) (%)		9.83±2	9.17 ±1.84	10.38 ±2.54
Organ Weight (g)	**Testis**	1.063±0.009	$0.927\pm0.007^{a***}$	$1.006\pm0.006^{ab***}$
	Prostate	0.231±0.003	$0.163\pm0.003^{a***}$	$0.207\pm0.003^{ab***}$
	Sem Ves	0.473±0.004	$0.327\pm0.006^{a***}$	$0.427\pm0.003^{ab***}$
	Epididymis	0.268±0.004	$0.231\pm0.003^{a***}$	$0.251\pm0.003^{a*b***}$
Gravimetric Index (g %)	**Testis**	0.834±0.004	$0.734\pm0.005^{a***}$	$0.792\pm0.01^{ab***}$
	Prostate	0.178±0.001	$0.129\pm0.002^{a***}$	$0.156\pm0.005^{ab***}$
	Sem Ves	0.37±0.003	$0.26\pm0.003^{a***}$	$0.33\pm0.002^{ab***}$
	Epididymis	0.211±0.001	$0.183\pm0.001^{a***}$	$0.199\pm0.002^{ab***}$

The data are presented as Mean ± SEM, (n=6). [a] designates control verses treated and supplement; [b] designates treated verses supplement. Level of significance; ***($p<0.001$). F-I denotes final - initial body weight

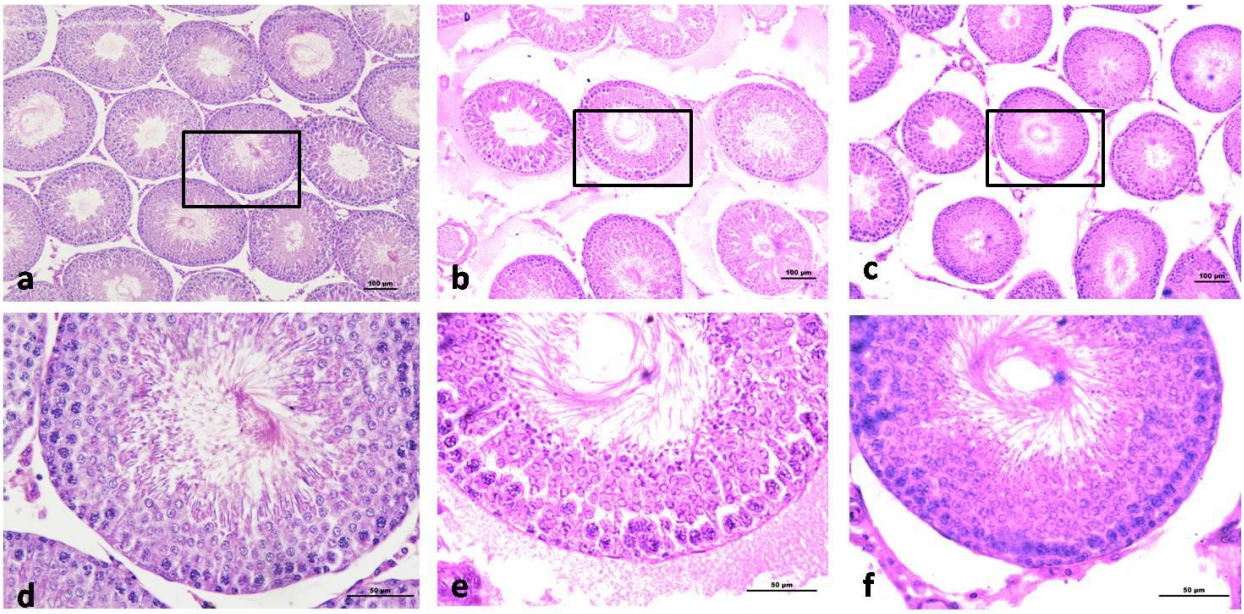

Figure 1 Photomicrograph of H/E stained testes of rats from all groups. Testis from control rat showed compactly arranged cellular array and alliance with numerous spermatozoa in the lumen; [a 100X & d 400X]. Testis from arsenic treated rat depicted disruption of cellular association with increase in luminal size, reduced sperm concentration along with presence of vacuoles; [b 100X & e 400X]. Testis from FHPD supplemented rat demonstrated normal orientation of the spermatogenic cell and huge presence of spermatozoa in the luminal area; [c 100X & f 400X].

Table 4 Effect of FHPD supplementation on testicular histomorphometry of arsenic treated adult rats

Parameters	Control (Gr - I)	Treated (Gr – II)	Supplement (Gr – III)
STD (µm)	269.72±2.60	$247.62\pm2.78^{a***}$	$260.76\pm2.19^{b**}$
LD (µm)	48.46±1.70	$68.67\pm1.19^{a***}$	$59.62\pm2.14^{a***b**}$
SEH (µm)	70.64±1.21	$50.83\pm0.95^{a***}$	$60.16\pm1.40^{a**b***}$
LCNA (μm^2)	38.26±0.61	$25.01\pm0.42^{a***}$	$32.20\pm0.44^{a**b***}$
SCN (10^6)	3.77±0.24	$2.34\pm0.15^{a***}$	$3.70\pm0.21^{b***}$
LCN (10^6)	5.78±0.23	$4.12\pm0.12^{a***}$	$5.31\pm0.17^{b***}$

The data are presented as Mean ± SEM, (n=6). [a] designates control verses treated and supplement; [b] designates treated verses supplement. Level of significance; **($p<0.01$), ***($p<0.001$). STD- Seminiferous tubule diameter, LD- Lumen diameter, SEH- Seminiferous epithelial height, LCNA- Leydig Cell nuclear area, SCN- Sertoli Cell number, LCN- Leydig Cell number

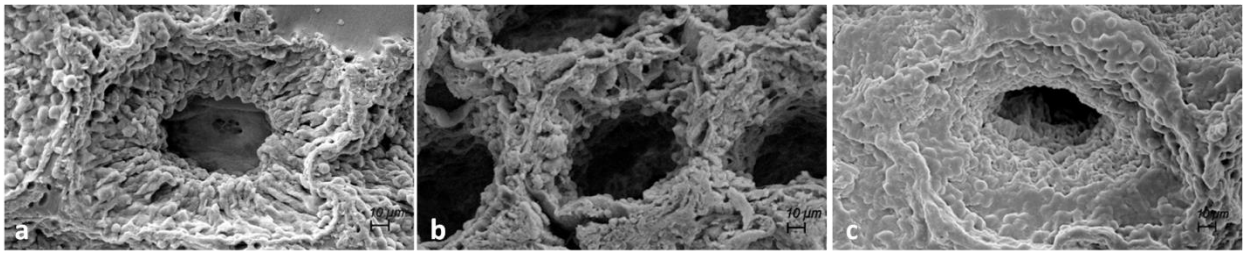

Figure 2 Scanning electron micrograph of testis from control rat sketched compact cellular assortment in seminiferous tubules; [a-(1.00 K X)]. The micrograph from arsenic exposed rat testis exhibited disorganized germinal layers in seminiferous tubules [b-(1.00 K X)]. The micrograph from FHPD supplemented rat testis revealed organized seminiferous tubules [c-(1.00 K X)].

Table 5 Effect of FHPD supplementation on spermatozoal potentials of arsenic exposed adult rats

Sperm Potentials		Control (Gr - I)	Treated (Gr – II)	Supplement (Gr – III)
Number (x10^6)		56.08±2.3	28.15±1.57^{a}***	45.83±0.85^{ab}***
Motility	**TMS (%)**	87.50±0.76	61.00±0.96^{a}***	71.83±1.1^{ab}***
	PMS (%)	71.33±0.49	39.83±0.47^{a}***	53.83±0.94^{ab}***
	NPMS (%)	16.16±0.47	21.16±0.60^{a}***	18.00±0.73^{ab}***
	NMS (%)	12.50±0.76	39.00±0.96^{a}***	28.16±1.10^{ab}***
Viability (%)		86.33±1.43	50.50±0.77^{a}***	68.33±0.88^{ab}***
HOS +ve (%)		70.56±0.42	44.05±0.51^{a}***	57.64±0.65^{ab}***

The data are presented as Mean ± SEM, (n=6). ^{a} designates control verses treated and supplement; ^{b} designates treated verses supplement. Level of significance; ***($p<0.001$). TMS- Total motile sperm, PMS- Progressive motile sperm, NMPS- Non progressive motile sperm, NMS- Non motile sperm and HOS- Hypoosmotic swelling.

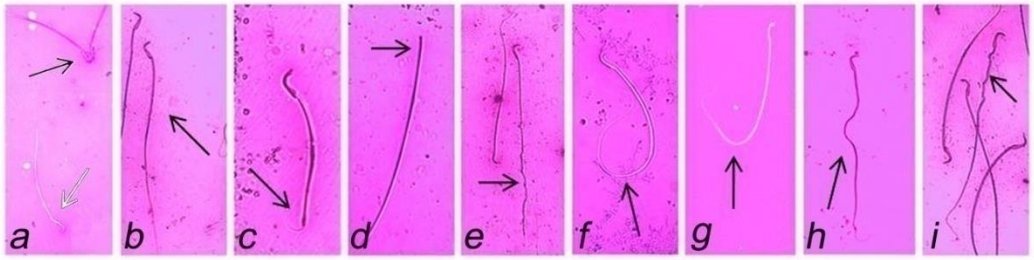

Figure 3 Eosin-nigrosin stained images of caudal spermatozoa (a-i) from arsenic treated rats. White arrow indicates live spermatozoa and black arrow represents dead spermatozoa (a). Normal spermatozoa (b), rudimentary tail (c), headless tail (d), bent tail (e), coiled tail (f), curved tail (g), curved midpiece (h) and bent midpiece (i) were the observed spermatozoal anomalies.

Table 6 Effect of FHPD supplementation on spermatozoal structural anomalies of spermatozoa in arsenic exposed adult rats

Structural anomalies			Control (Gr - I)	Treated (Gr – II)	Supplement (Gr – III)
Morphology (%)	**Primary**	**RT**	1.50 ± 0.22	3.16 ± 0.17^{a}***	2.33±0.21^{a}*^{b}*
	Secondary	**HT**	2.67 ± 0.33	4.33 ± 0.33^{a}**	2.50±0.34^{b}**
		BT	1.50 ± 0.22	2.83 ± 0.30^{a}**	2.33±0.2^{a}*
		COT	1.83 ± 0.17	3.00 ± 0.26^{a}**	2.50±0.22^{a}*
		CUT	1.17 ± 0.17	2.66 ± 0.21^{a}***	2.50±0.22^{a}***
		CMP	1.67 ± 0.21	2.67 ± 0.33^{a}*	2.50±0.22^{a}*
		BMP	1.67 ± 0.21	2.83 ± 0.30^{a}**	2.33±0.21
	Total abnormal cells		12.00 ± 0.73	21.50 ±0.42^{a}***	17.00±0.58^{ab}***

The data are presented as Mean ± SEM, (n=6). ^{a} designates control verses treated and supplement; ^{b} designates treated verses supplement. Level of significance; *($p<0.05$), **($p<0.01$), ***($p<0.001$). RT- round tail, HT- headless tail, BT- bent tail, COT- coiled tail, CUT- curve tail, BMP- bent mid piece

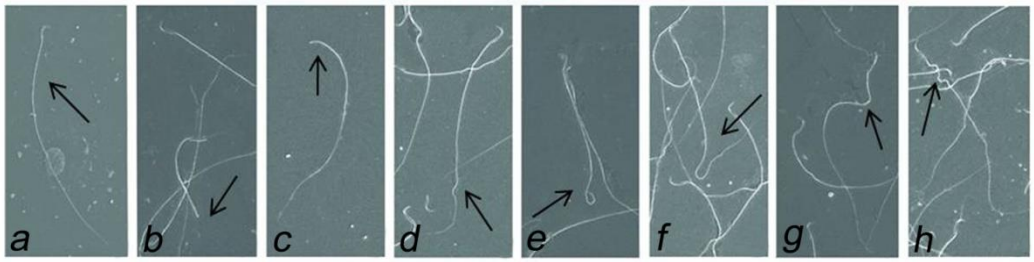

Figure 4 Scanning electron micrographs of caudal spermatozoa (a-h) from arsenic treated rats. Normal spermatozoa (a), rudimentary tail (b), headless tail (c), bent tail (d), coiled tail (e), curved tail (f), curved midpiece (g) and bent midpiece (h) were the observed spermatozoal anomalies.

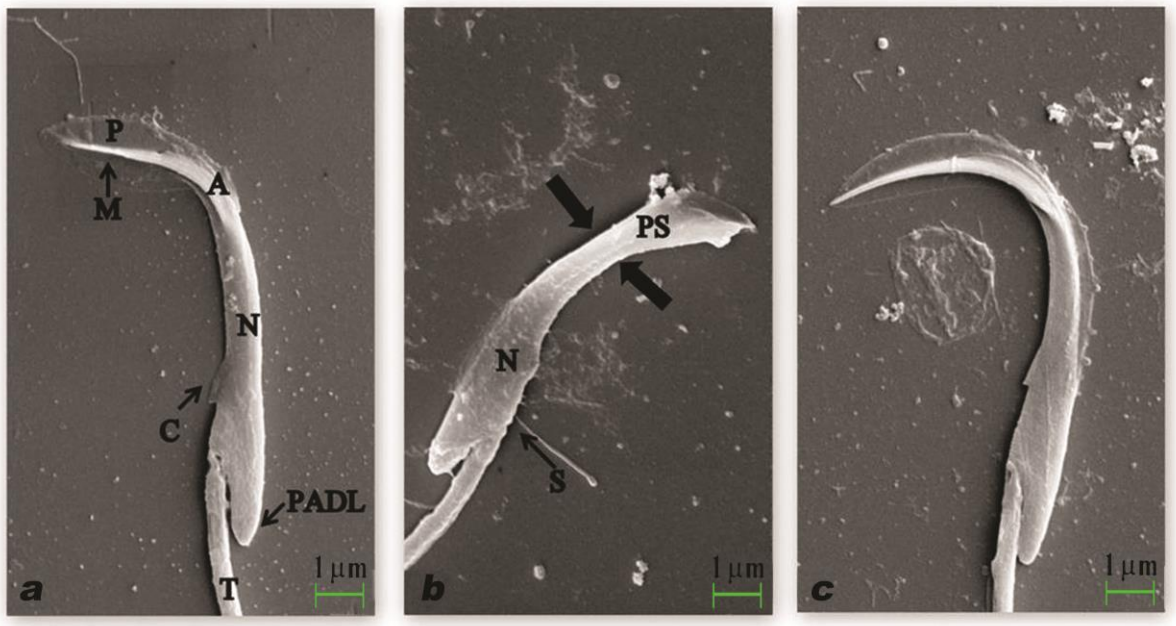

Figure 5 Scanning electron micrographs (15.00 KX) of head region of caudal spermatozoa from control (a), arsenic exposed (b) and FHPD supplemented (c) rats. (a) Spermatozoa of control rat exhibited normal features like intact acrosome (A); post nuclear cap (C); plasma membrane (M); nucleus (N); perforatium (subacrosomal material) (P); post acrosomal dense laminar region (PADL) and tail region (T). (b) The swelled perforatium (PS) and dorsoventrally constriction at the mid region (arrow) of the head, serrations at the connective piece (S) and distorted post nuclear cap (C) were noted in arsenic treated spermatozoa. Shortening in the length of post acrosomal dense laminar region (PADL) is also noted. (c) Spermatozoa of FHPD supplemented rat displayed nearly normal structure to that of control rat.

Table 7 Effect of FHPD supplementation on ultra-structure of spermatozoal head on arsenic exposed adult rats

Parameter	Control (Gr - I)	Treated (Gr – II)	Supplement (Gr – III)
Spermatozoal head deformity %	14.90±0.82	31.44±1.49[a]***	22.94±0.95[ab]***

The data are presented as Mean ± SEM, (n=6). [a] designates control verses treated and supplement; [b] designates treated verses supplement. Level of significance; ***($p<0.001$).

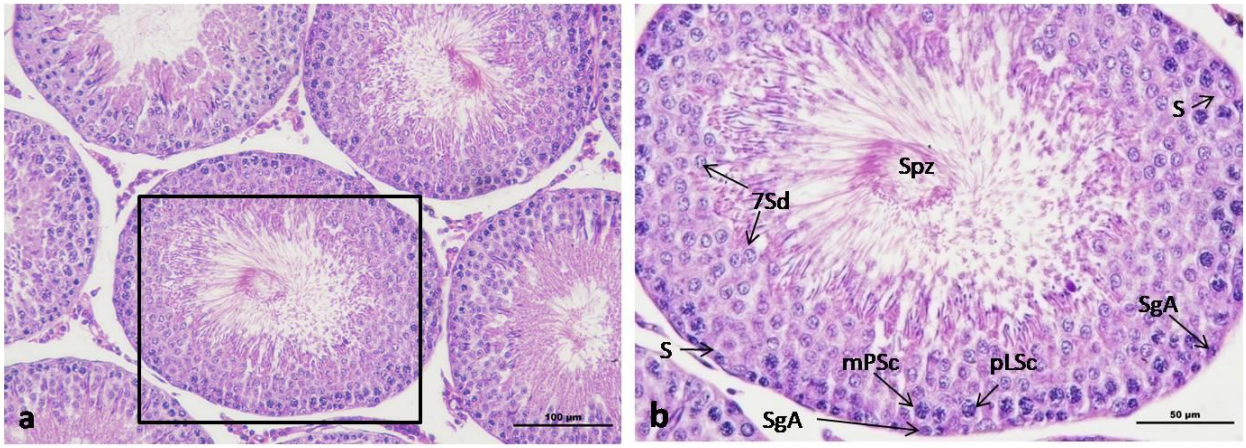

Figure 6 Photomicrograph of H/E stained control testis depicting arrangement of different spermatogonial cell at stage VII spermatogenic cycle, needed for spermatokinetics study; [a (200X) & b (400X)]. SgA- Spermatogonia A, pLSc- Preleptotene Spermatid, mPSc- Mid-pachytene Spermatid, 7Sd- Step 7 Spermatid, S- Sertoli cell, Spz- Spermatozoa.

Table 8 Effect of FHPD supplementation on spermatogenic growth studied at stage VII spermatogenic cycle in arsenic treated adult rats

Parameters	Parameters	Control (Gr - I)	Treated (Gr – II)	Supplement (Gr – III)
Spermato-kinetics (10^6)	**SgA**	0.747±0.0139	0.460±0.0086^{a}***	0.637±0.0316^{a}**^{b}***
	pLSc	17.39±0.10	12.58±0.14^{a}***	16.41±0.09^{ab}**
	mPSc	18.09±0.05	12.80±0.08^{a}***	17.56±0.08^{ab}**
	7Sd	62.97±0.78	39.88±0.17^{a}***	59.54±0.18^{ab}***
Derived data	**mPSc:7Sd**	1:3.48	1:3.11	1:3.39
	7Sd degeneration %	14.91	28.38	18.47
	Effective 7Sd degeneration	-	+13.47	+3.56

The data are presented as Mean ± SEM, (n=6). [a] designates control verses treated and supplement; [b] designates treated verses supplement. Level of significance; **($p<0.01$), ***($p<0.001$). SgA- Spermatogonia A, pLSc- Preleptotene Spermatid, mPSc- Mid-pachytene Spermatid, 7Sd- Step 7 Spermatid.

Table 9 Effect of FHPD supplementation on the activity of testicular marker enzymes in arsenic treated adult rats

Parameters	Control (Gr - I)	Treated (Gr – II)	Supplement (Gr – III)
LDH (units/mg protein)	0.76±0.017	1.27±0.020^{a}***	0.90±0.011^{ab}***
γ-GT (units/mg protein)	0.29±0.007	0.17±0.007^{a}***	0.23±0.004^{ab}***
ACP (µg PNP/mg tissue/ hr)	25.72±0.26	31.99±0.31^{a}***	28.74±0.24^{ab}***
ALP (µg PNP/mg tissue/ hr)	19.79±0.24	27.49±0.28^{a}***	22.13±0.26^{ab}***

The data are presented as Mean ± SEM, (n=6). [a] designates control verses treated and supplement; [b] designates treated verses supplement. Level of significance; ***($p<0.001$). LDH- Lactate dehydrogenase, γ-GT- Gamma glutamyl transferase, ACP- Acid phosphatase, ALP- Alkaline Phosphatase

Table 10 Effects of FHPD supplementation on the activity of testicular key regulatory steroidogenic enzymes and serum testosterone level in arsenic exposed adult rats

Parameters	Control (Gr - I)	Treated (Gr – II)	Supplement (Gr – III)
Δ^5 3β HSD (units/mg of tissue/hr)	5.57±0.34	3.11±0.64^{a}**	5.29±0.48^{b}*
17β HSD (units/mg of tissue/hr)	5.41±0.36	2.94±0.37^{a}*	5.42±0.93^{b}*
Testosterone (ng/ml serum)	1.21±0.06	0.77±0.02^{a}***	1.24±0.05^{b}***

The data are presented as Mean ± SEM, (n=6). [a] designates control verses treated and supplement; [b] designates treated verses supplement. Level of significance; *($p<0.05$), **($p<0.01$), ***($p<0.001$)

Table 11 Effect of FHPD supplementation on non-enzymatic oxidative stress parameters in arsenic exposed adult rats

Oxidative stress parameters		Control (Gr - I)	Treated (Gr – II)	Supplement (Gr – III)
Nonenzymatic	**MDA (nM/mg tissue)**	24.5±0.17	47.06±2.6[a]***	25.05±3.93[b]***
	PC (µM/mg protein)	25.05±1.31	38.89±1.17[a]***	28.9±0.91[ab]***
	GSH (µM/mg tissue)	665.7±39	406.5±34.2[a]***	658.0±62.9[b]***

The data are presented as Mean ± SEM, (n=6). [a] designates control verses treated and supplement; [b] designates treated verses supplement. Level of significance; ***($p<0.001$). MDA- Malondialdehyde, PC- Protein carbonyl, GSH- Reduced glutathione

Table 12 Effect of FHPD supplementation on enzymatic oxidative stress parameters in arsenic exposed adult rats

Oxidative stress parameters		Control (Gr - I)	Treated (Gr – II)	Supplement (Gr – III)
Enzymatic	**SOD (unit/mg tissue)**	1.464±0.02	0.919±0.03[a]***	1.328±0.07[a]***
	Catalase (µM H202 consumption/mg of tissue/min)	133.6±2.14	57.48±2.78[a]***	123.7±2.3[ab]***
	GST (µM NADPH consumed/min/mg protein)	33.81±1.03	23.28±0.45[a]***	32.07±2.11[b]***
	GPx (µM NADPH oxidized/mg tissue/minute)	23.4±0.82	16.13±0.86[a]***	22.76±0.78[b]***
	GR(µM NADPH/min)	24.04±0.91	15.7±0.86[a]***	23.77±0.96[b]***

The data are presented as Mean ± SEM, (n=6). [a] designates control verses treated and supplement; [b] designates treated verses supplement. Level of significance; ***($p<0.001$). SOD- Superoxide dismutase, GST- Glutathione S-transferase, GPx- Glutathione peroxidase, GR- Glutathione reductase.

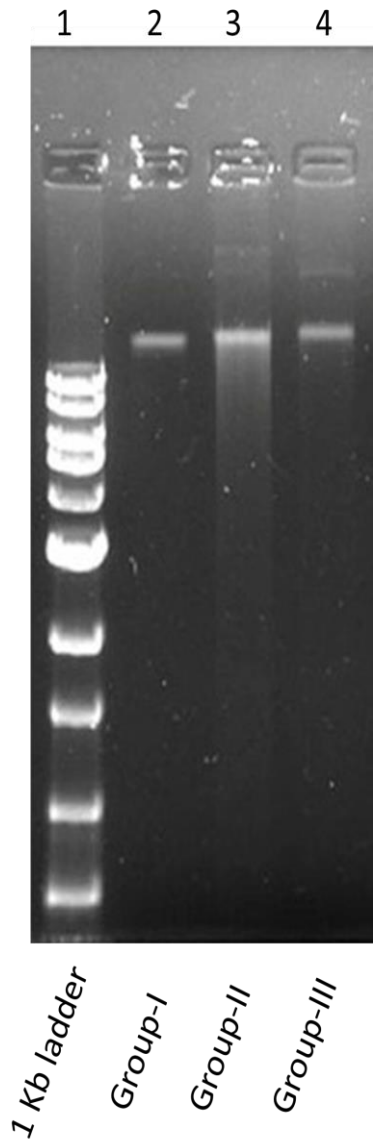

Figure 7 Photomicrograph of the testicular DNA fragmentation of experimental rats in agarose gel electrophoresis. Lane 1 indicated 1kb DNA ladder; Lane 2 denoted single band of testicular DNA from control group; Lane 3 represented single band with salient trailing of fragmented testicular DNA from arsenic exposed group; Lane 4 specified single band of testicular DNA with no trailing from supplemented group.

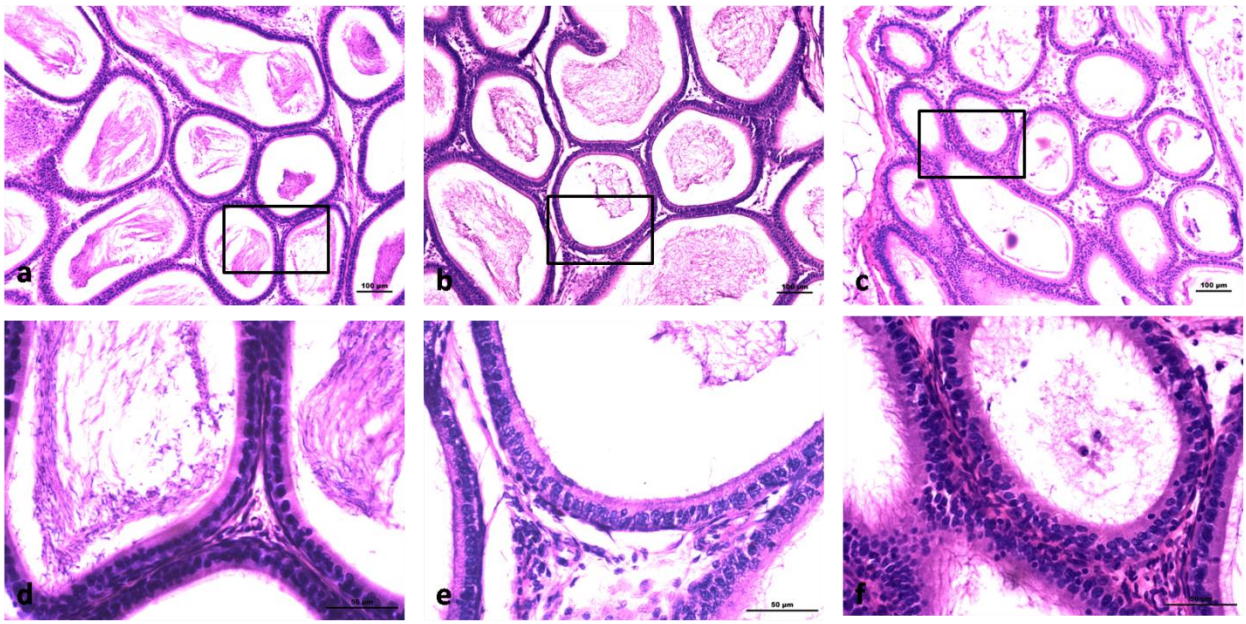

Figure 8 Photomicrograph of the cauda epididymis in experimental rats. H/E stained cauda epididymis from control rat portrayed normal tubular architecture, presence of stereocilia and lumen occupied with spermatozoa; [a 100X & d 400X]. H/E stained cauda epididymis from arsenic treated rat revealed thinning of tubular architecture, absence of stereocilia and lesser concentration of spermatozoa in the lumen; [b 100X & e 400X]. H/E stained cauda epididymis from FHPD supplemented rat illustrated restoration of tubular shape, presence of stereocilia and lumen occupied with spermatozoa; [c 100X & f 400X].

Table 13 Effect of FHPD supplementation on non-enzymatic and enzymatic oxidative stress parameters of arsenic exposed cauda epididymis in adult rats

Oxidative stress parameters		Control (Gr - I)	Treated (Gr – II)	Supplement (Gr – III)
Non-enzymatic	**MDA (nM/mg tissue)**	21.4±1.81	39.05±1.77[a]***	22.29±2.08[b]***
	PC (µM/mg protein)	19.51±1.62	32.16±1.81[a]***	20.98±1.33[b]***
Enzymatic	**SOD (unit/mg tissue)**	1.223±0.03	0.764±0.02[a]***	1.204±0.03[b]***
	Catalase (µM H_20_2 consumption/mg of tissue/min)	114.5±2.6	76.1±2.72[a]***	106.9±2.89[b]***

The data are presented as Mean ± SEM, (n=6). [a] designates control verses treated and supplement; [b] designates treated verses supplement. Level of significance; ***($p<0.001$). MDA-Malondialdehyde, PC- Protein carbonyl, SOD- Superoxide dismutase.

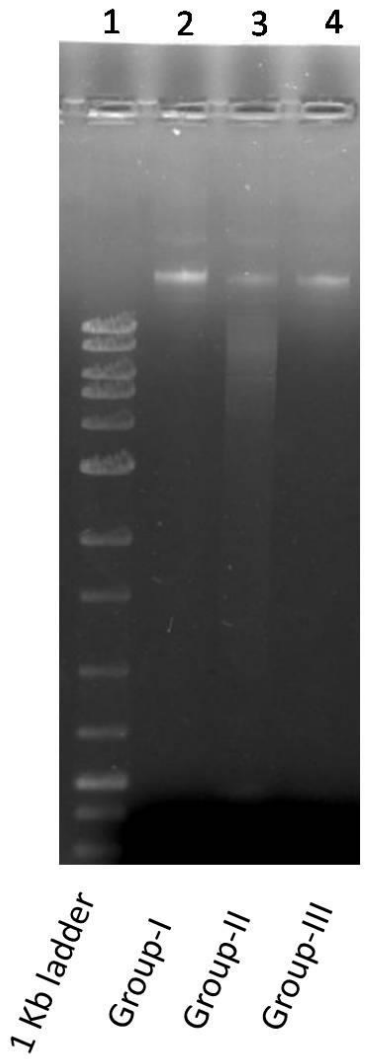

Figure 9 Photomicrograph of the DNA fragmentation of cauda epididymis of experimental rats in agarose gel electrophoresis. Lane 1 referred to 1kb DNA ladder; Lane 2 showed single band of cauda epididymis DNA from control group; Lane 3 represented single band with salient trailing of fragmented cauda epididymis DNA from arsenic exposed group; Lane 4 denoted single band of cauda epididymis DNA with no trailing of genomic DNA from supplemented group.

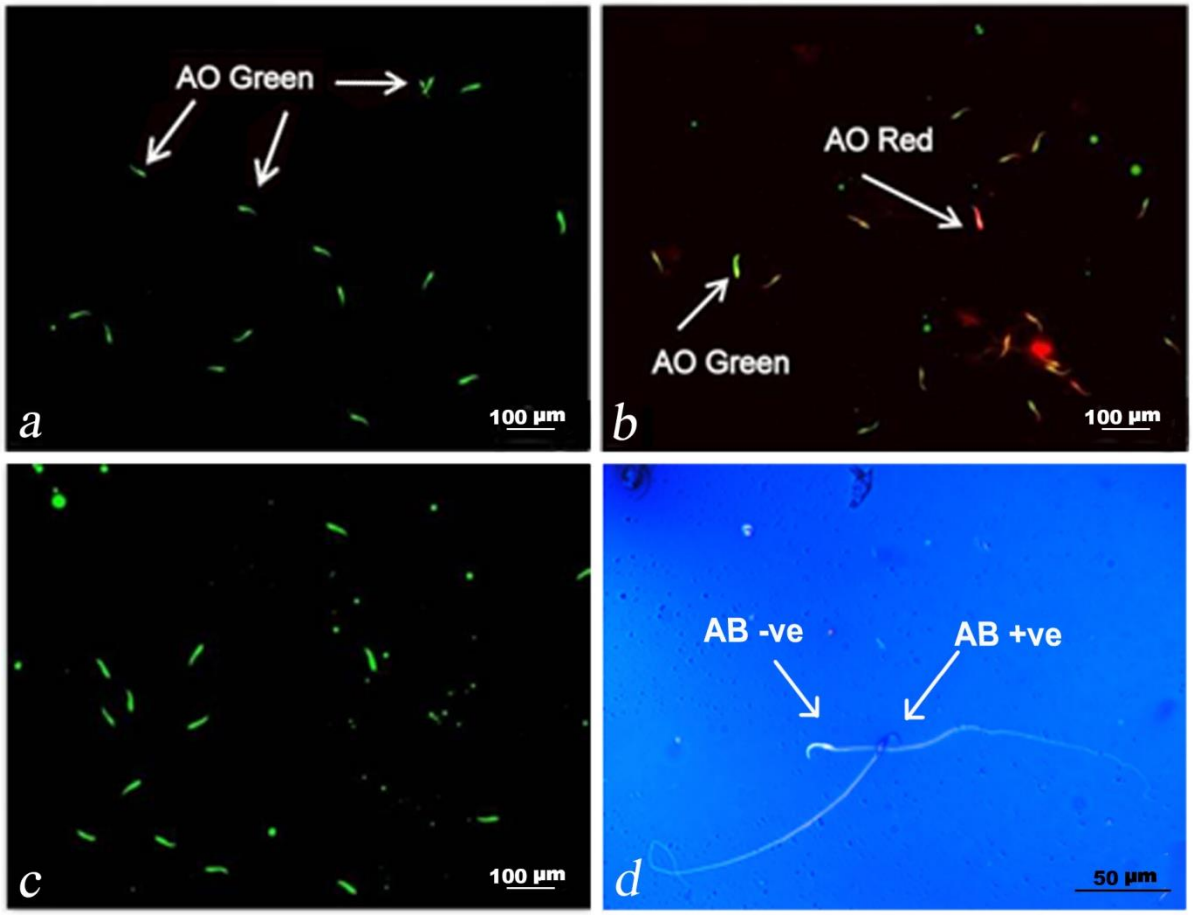

Figure 10 Photomicrograph (100X) of acridine orange stained caudal spermatozoa in control (a), arsenic exposed (b) and FHPD supplemented (c) rats. AO-green indicates spermatozoa with native double stranded DNA and AO-red indicates damaged single stranded DNA. Photomicrograph (400X) of aniline blue stained caudal spermatozoa showing deep blue (AB+ve) head indicate immature spermatozoa while colourless (AB-ve) head denotes mature one (d).

Table 14 Effect of FHPD supplementation on DNA status and maturity in arsenic treated adult rats

Spermatozoal maturity		Control (Gr - I)	Treated (Gr – II)	Supplement (Gr – III)
DNA Status (%)	AO Green (%)	86.48±0.69	$56.70\pm1.38^{a***}$	$76.16\pm1.11^{ab***}$
	AB+ve (%)	15.18±0.49	$40.34\pm0.91^{a***}$	$29.02\pm0.51^{ab***}$

The data are presented as Mean ± SEM, (n=6). [a] designates control verses treated and supplement; [b] designates treated verses supplement. Level of significance; ***($p<0.001$). AO- acridine orange, AB- aniline blue

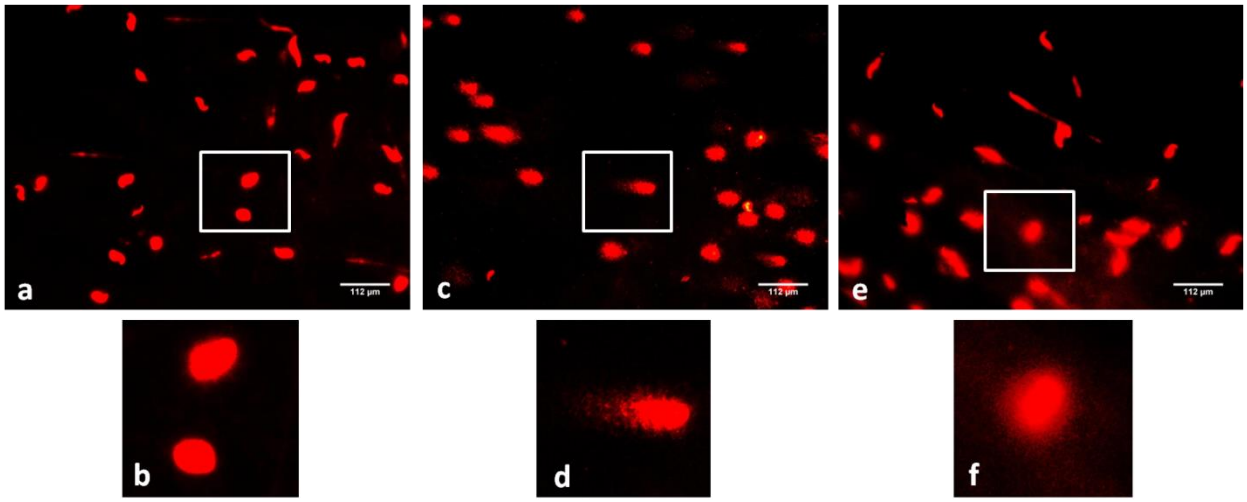

Figure 11 Photomicrograph of spermatozoal comet assay in control [a & b] arsenic exposed (c & d) and FHPD supplemented (e & f) rats by single-cell gel electrophoresis [100X and enlarged].

Table 15 Effect of FHPD supplementation on spermatozoal DNA damage in arsenic intoxicated adult rats

Sperm DNA damage (%)	Parameters	Control (Gr - I)	Treated (Gr – II)	Supplement (Gr – III)
Comet assay	**% Head DNA**	97.59±0.45	86.10±1.35^{a}***	95.59±0.59^{b}***
	% Tail DNA	2.40±0.45	13.81±1.30^{a}***	4.39±0.59^{b}***
	% Tail movement	0.168±0.070	1.00±0.238^{a}***	0.228±0.028^{b}**
	% Olive tail movement	0.566±0.272	1.86±0.479^{a}*	0.697±0.147^{b}*

The data are presented as Mean ± SEM, (n=6). ^{a} designates control verses treated and supplement; ^{b} designates treated verses supplement. Level of significance; *($p<0.05$), **($p<0.01$), ***($p<0.001$)

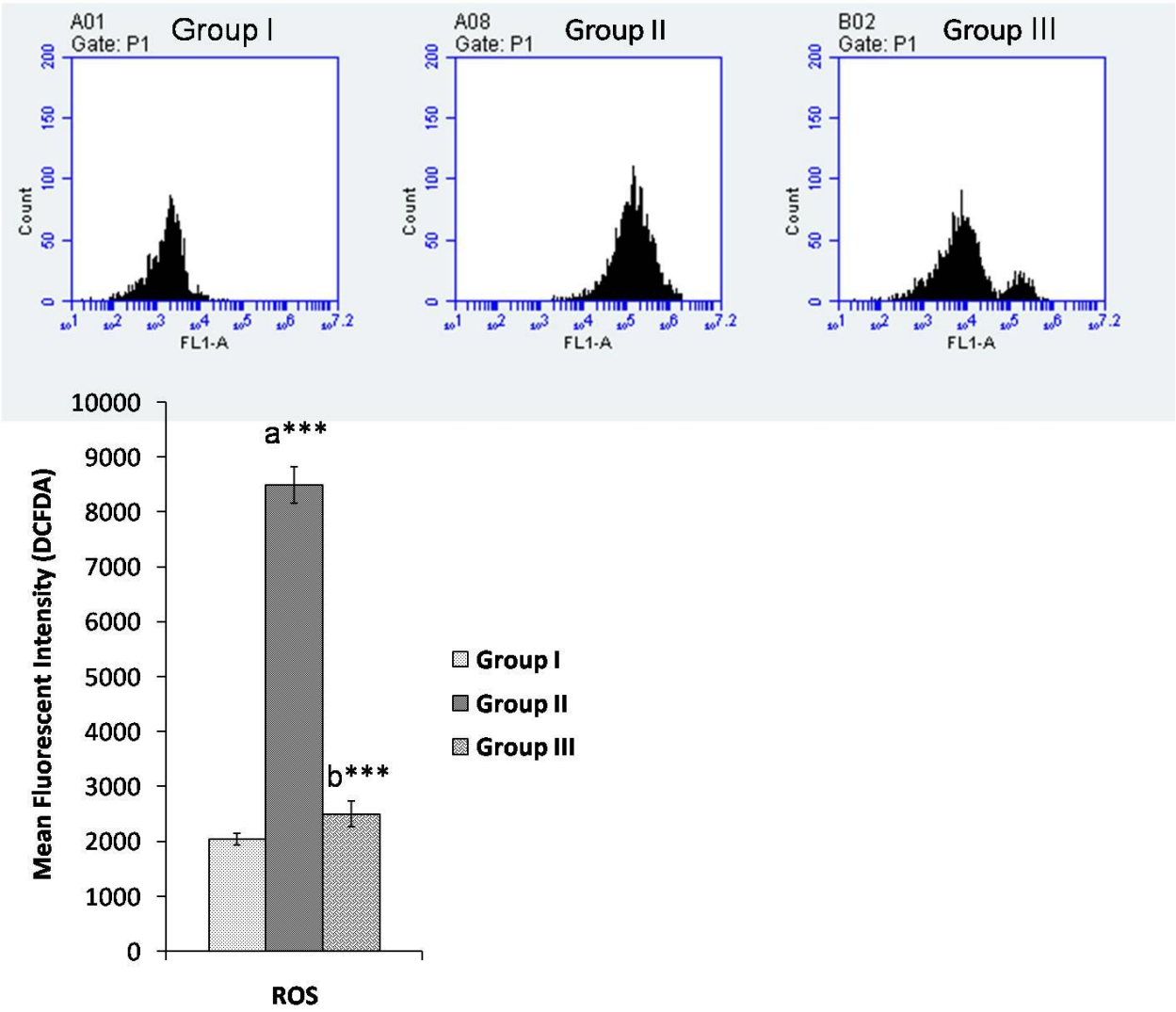

Figure 12 Effect of FHPD on arsenic induced spermatozoal ROS generation by flow cytometric analysis using DCFDA. The data are presented as Mean ± SEM, (n=6). [a] designates control verses treated and supplement; [b] designates treated verses supplement. Level of significance; ***($p<0.001$)

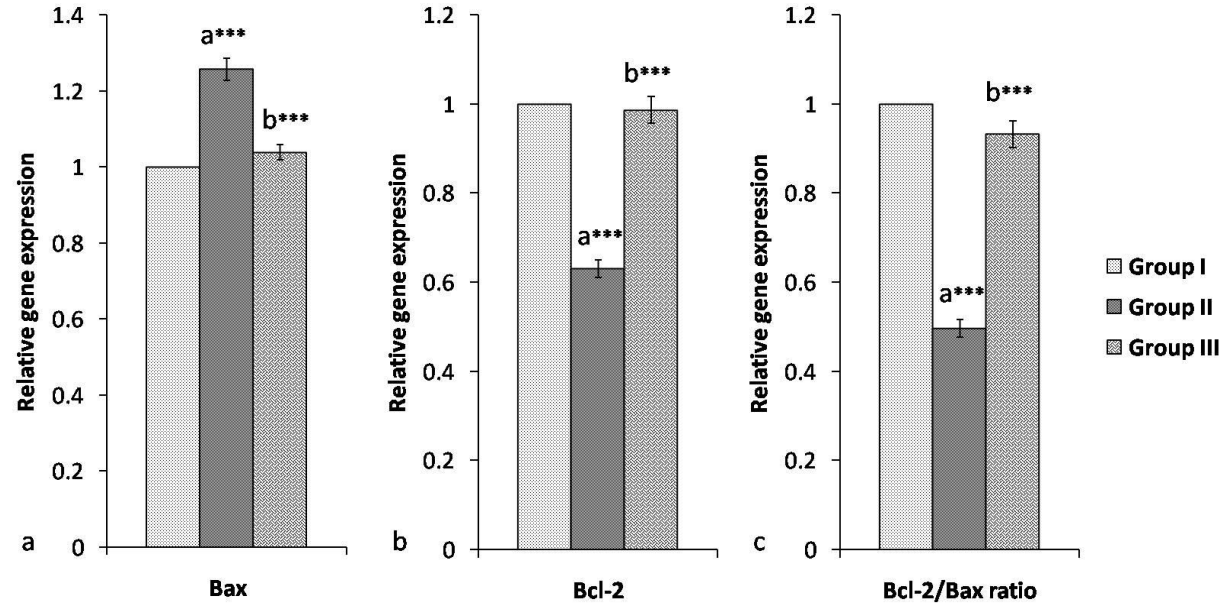

Figure 13 Bar diagram illustrating analysis of relative gene expression of Bax (a), Bcl-2 (b) and Bcl-2/Bax ratio (c) from testes in control and experimental rats. The data are presented as Mean ± SEM, (n=6). [a] designates control verses treated and supplement; [b] designates treated verses supplement. Level of significance; ***($p<0.001$)

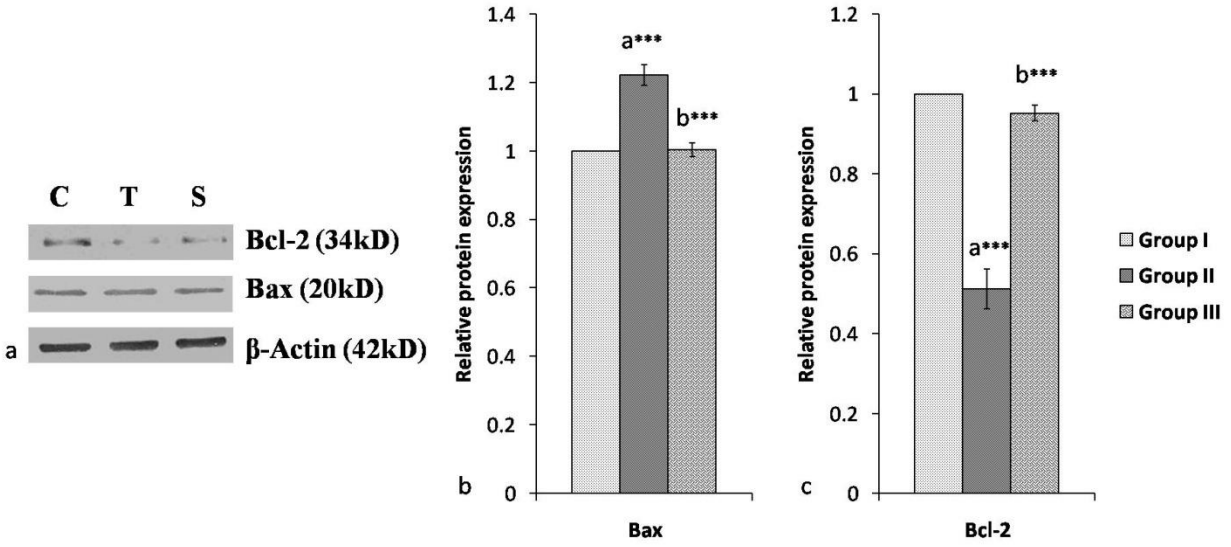

Figure 14 Testicular protein level expressions of Bax and Bcl-2 analyzed by Western Blotting and its densitometric analysis. β-actin was used as loading control and densitometric analysis was done with reference to corresponding band of β-actin expression. (a) indicates band intensities of respective group where C is Group-I; T is Group-II and S is Group-III. (b) and (c) indicates relative protein expression of Bax and Bcl-2 respectively. The data are presented as Mean ± SEM, (n=6). [a] designates control verses treated and supplement; [b] designates treated verses supplement. Level of significance; ***($p<0.001$)

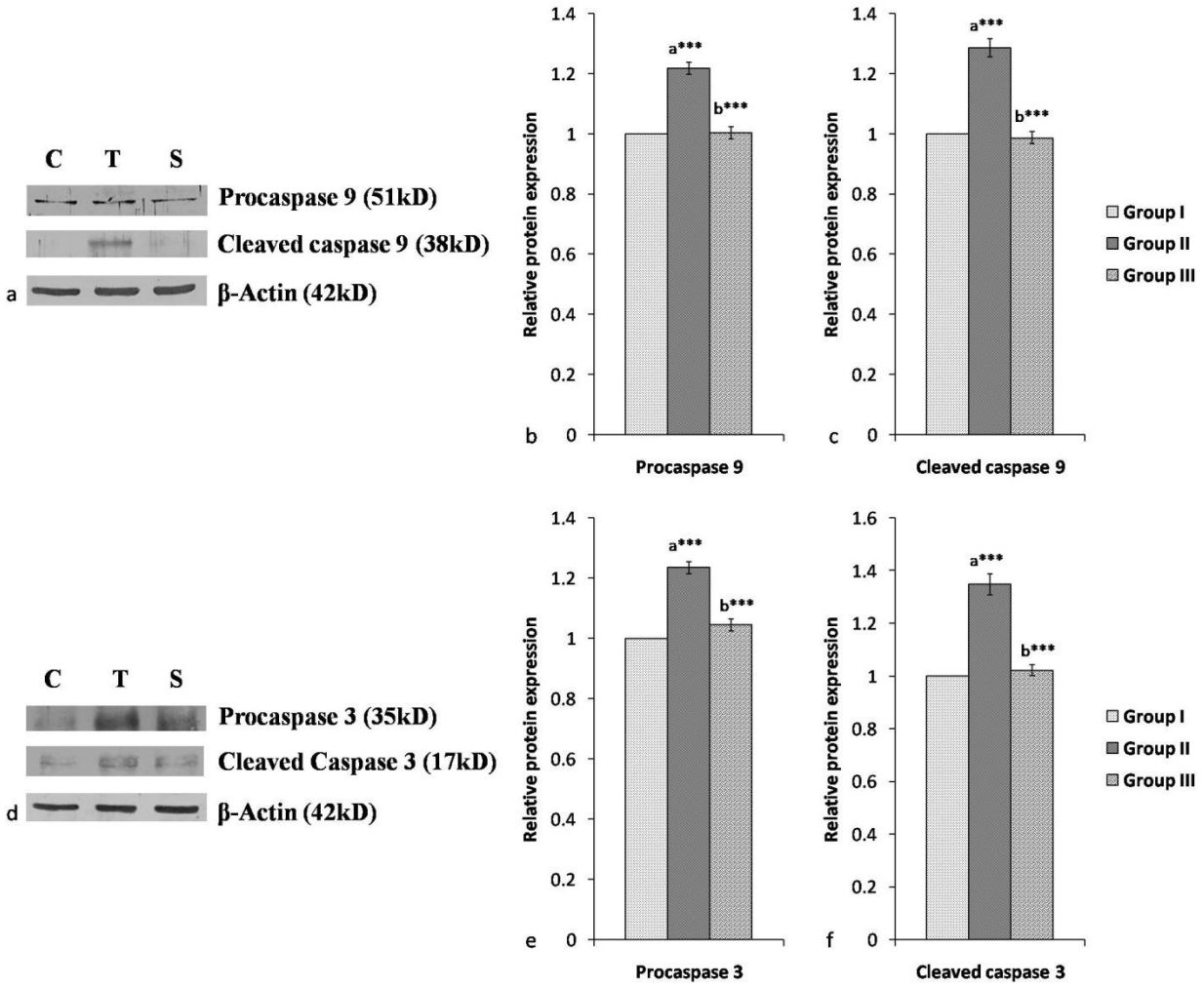

Figure 15 Testicular protein level expressions of procaspase 9, cleaved caspase 9, procaspase 3 and cleaved caspase 3 analyzed by Western Blotting and its densitometric analysis. β-actin was used as loading control and densitometric analysis was done with reference to corresponding band of β-actin expression. (a) and (d) indicate band intensities of respective group where C is Group-I; T is Group-II and S is Group-III. (b), (c), (e) and (f) indicate relative protein expression of procaspase 9, cleaved caspase 9, procaspase 3 and cleaved caspase 3 respectively. The data are presented as Mean±SEM, (n=6). [a] designates control verses treated and supplement; [b] designates treated verses supplement. Level of significance; ***($p<0.001$)

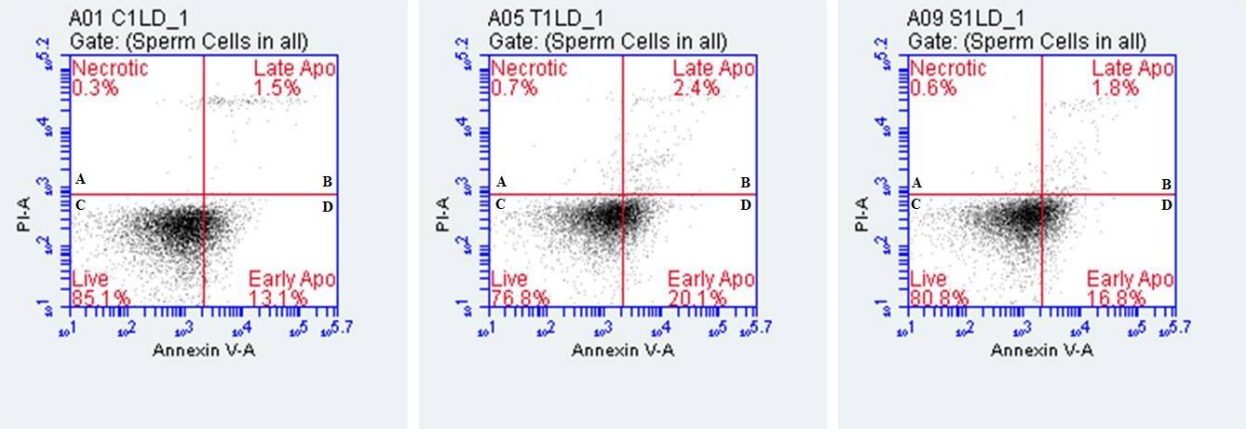

Figure 16 The flow cytometric profile of epididymal spermatozoa in control, arsenic treated and FHPD supplemented rats that are labeled with Annexin V and PI. A) Necrotic cells. B) Late apoptotic cells. C) Fully viable cells. D) Early Apoptotic cells.

Table 16 Effect of FHPD supplementation on spermatozoal apoptosis caused by arsenic toxicity in adult male rats

Parameters	**Control (Gr -I)**	**Treated (Gr- II)**	**Supplemented (Gr- III)**
Early apoptotic spermatozoa %	12.75±0.127	19.65±0.164^{a}***	16.90±0.365^{ab}***
Late apoptotic spermatozoa %	1.45±0.018	2.65±0.091^{a}***	1.76±0.021^{a}**^{b}***
Necrotic spermatozoa %	0.33±0.021	0.70±0.036^{a}***	0.60±0.036^{a}***^{b}*

The data are presented as Mean ± SEM, (n=6). ^{a} designates control verses treated and supplement; ^{b} designates treated verses supplement. Level of significance; *($p<0.05$), **($p<0.01$), ***($p<0.001$)

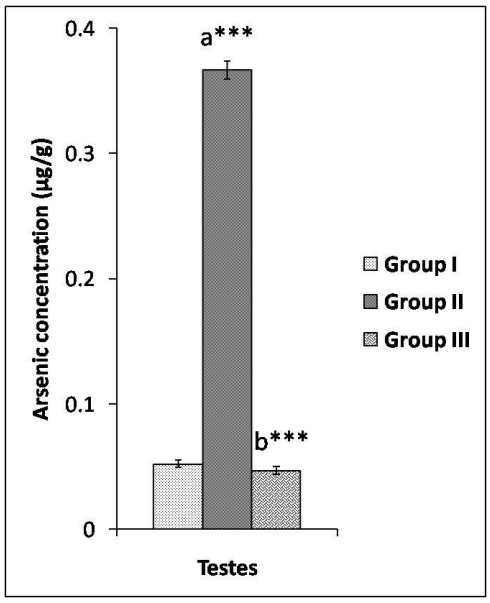

Figure 17 Bar diagram depicting testicular arsenic concentration (ppb) in control and experimental rats. The data are presented as Mean ± SEM, (n=6). [a] designates control verses treated and supplement; [b] designates treated verses supplement. Level of significance; ***($p<0.001$)

Curiginal

Document Information

Analyzed document	Sagnik Biswas 5000 words revised urkund 110921.docx (D112501622)
Submitted	9/13/2021 4:59:00 PM
Submitted by	Rabishankar Giri
Submitter email	rabi.lib@presiuniv.ac.in
Similarity	4%
Analysis address	rabi.lib.presi@analysis.urkund.com

Sources included in the report

W	URL: https://pubmed.ncbi.nlm.nih.gov/32196711/ Fetched: 9/13/2021 5:00:00 PM	1
W	URL: http://globalresearchonline.net/journalcontents/v26-2/48.pdf Fetched: 9/13/2021 5:00:00 PM	2
J	URL: 40e25014-9178-4490-ac6f-da5df1ebea2c Fetched: 2/26/2020 3:22:56 PM	6
J	URL: 10ea138b-c6d1-41eb-8ebe-40465197d67c Fetched: 11/2/2019 3:20:58 AM	1
W	URL: https://www.researchgate.net/publication/320862485_Testicular_toxicity_and_sperm_quality_following_copper_exposure_in_Wistar_albino_rats_ameliorative_potentials_of_L-carnitine Fetched: 5/5/2021 10:55:31 AM	1
W	URL: https://www.degruyter.com/document/doi/10.1515/jbcpp-2012-0039/html Fetched: 9/13/2021 5:00:00 PM	1

MINISTRY OF ENVIRONMENT AND FORESTS

CPCSEA

Government of India, New Delhi

Certificate of Appreciation

This is to certify that Prof. / Dr./ Ms. /Mr. Sagnik Biswas *of* Presidency University, Kolkata *has participated in the "Role of CPCSEA in Animal Welfare" workshop held on 2nd August, 2014, organized by CPCSEA, Animal Ethics Society of India, Indian Pharmacological Society and West Bengal University of Animal & Fishery Sciences at Department of Pharmacology & Toxicology, West Bengal University of Animal & Fishery Sciences, Belgachia, Kolkata.*

Dr. K.P. Mohanakumar
Chairman, Organizing Committee
Indian Institute of Chemical Biology
Govt. of India

Smt. M. Geethanjali
Member Secretary, CPCSEA
Ministry of Environment & Forests
New Delhi

Dr. B. Dinesh Kumar
President
Indian Pharmacological Society

Prof. T. K. Mandal
Organizing Secretary
WBUAFS, Kolkata

Scanned by TapScanner

Department of Biological Sciences

Presidency University, Kolkata

National Symposium on

"Molecules to Systems"

Certificate

This is to certify that Prof./ Dr./ Mr./ Ms.

Sagnik Biswas

of DBS, Presidency University, Kolkata

participated and presented a poster in the 1st National Symposium on "Molecules to Systems" at the Department of Biological Science, Presidency University held during 29th-31st January, 2015.

Head ,DBS

Convener

Scanned by TapScanner

Department of Zoology, University of Calcutta

INTZOOCON 2018

an International Conference to celebrate 100 years of excellence from 1919-2019
at the
Ramakrishna Mission Institute of Culture
& University of Calcutta (Ballygunge Campus)

February 1-3, 2018

Certificate of appreciation

This to certify that Prof./Dr./Mr./Mrs./Ms. Sagnik Biswas

participated in the International Conference as a Delegate/ Presenter of a Paper entitled Dietary High Proteins Ameliorate Arsenic-Mediated Testicular Disorders In Adult Rats.

Parthiba Basu & Sagartirtha Sarkar
Jt. Secretaries

Urmi Chatterji
President

Scanned by TapScanner

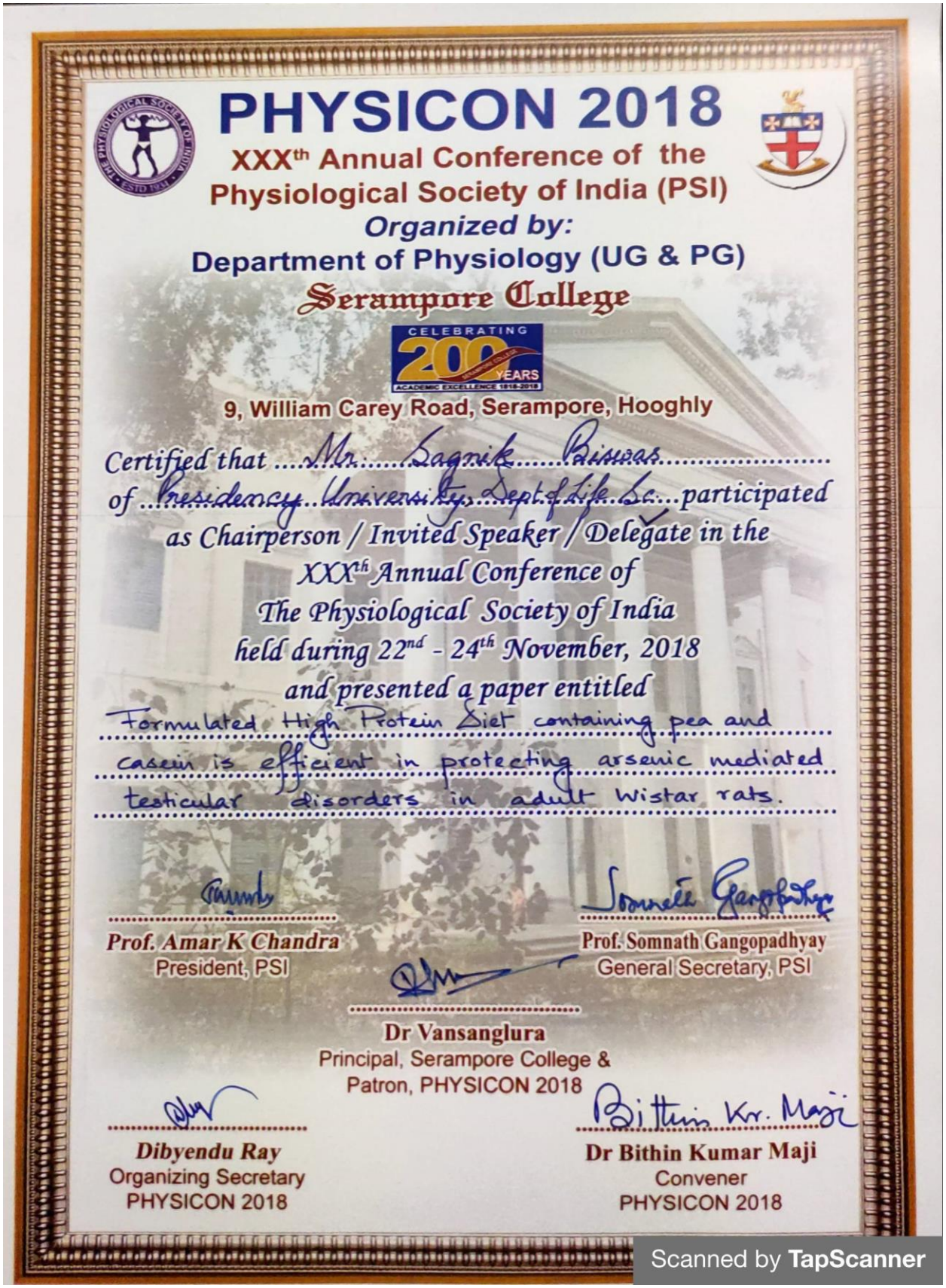

PHYSICON 2018

XXXth Annual Conference of the Physiological Society of India (PSI)

Organized by:

Department of Physiology (UG & PG)

Serampore College

CELEBRATING 200 YEARS

ACADEMIC EXCELLENCE 1818-2018

9, William Carey Road, Serampore, Hooghly

Certified that Mr. Sagnik Biswas

of Presidency University, Dept of Life Sc. *participated as Chairperson / Invited Speaker / Delegate in the XXXth Annual Conference of The Physiological Society of India held during 22nd - 24th November, 2018 and presented a paper entitled*

Formulated High Protein Diet containing pea and casein is efficient in protecting arsenic mediated testicular disorders in adult Wistar rats.

Prof. Amar K Chandra
President, PSI

Prof. Somnath Gangopadhyay
General Secretary, PSI

Dr Vansanglura
Principal, Serampore College &
Patron, PHYSICON 2018

Dibyendu Ray
Organizing Secretary
PHYSICON 2018

Dr Bithin Kumar Maji
Convener
PHYSICON 2018

Scanned by TapScanner

CERTIFICATE of PARTICIPATION

This is to certify that ***Sagnik Biswas*** *of Presidency University has participated in the workshop on Flow Cytometry Organized by Bio-Rad Laboratories from 26-08-2019 to 30-08-2019 .*

Dr. Rajesh Saha
Senior Field Application Scientist
Bio-Rad Laboratories

Lin Zhu
Global Field Application Scientist
Bio-Rad Laboratories

Dr. Nabendu Biswas
Assistant Professor
Presidency University

BIO-RAD

Scanned by TapScanner

Received: 24 November 2019 | Revised: 15 January 2020 | Accepted: 11 February 2020

DOI: 10.1111/and.13560

Check for updates

ORIGINAL ARTICLE

ANDROLOGIA WILEY

Casein- and pea-enriched high-protein diet can take care of the reprotoxic effects of arsenic in male rats

Sagnik Biswas | Prabir Kumar Mukhopadhyay

Department of Life Sciences, Presidency University, Kolkata, India

Correspondence
Prabir Kumar Mukhopadhyay, Department of Life Sciences, Presidency University, 86/1 College Street, Kolkata-700073, India.
Email: prabir.dbs@presiuniv.ac.in

Funding information
FRPDF fund of Presidency University

Abstract

Arsenic toxicity is a significant health problem featured with several incidents of male reproductive dysfunctions. We studied the protective effects of a casein- and pea-enriched formulated high-protein diet (FHPD) on arsenic-mediated testicular dysfunctions in rats. Adult male rats sustained on either a benchmark diet ($n = 8$) or an isocaloric FHPD ($n = 8$) were gavaged with arsenic trioxide (3mg/kg body wt/rat/day) for 30 consecutive days. A vehicle-fed group ($n = 8$) maintained on the standard diet served as control. The arsenic-treated group continued on the standard diet had a significantly reduced testicular and accessory sex organs weights. They exhibited decreased count, motility, viability and disrupted plasma membrane integrity of caudal spermatozoa with a higher incidence of gross morphological anomalies and DNA damage. Attenuated steroidogenic enzyme activities and low serum testosterone level vouched for a compromised state of testicular steroidogenesis. An increased testicular malondialdehyde and protein carbonyl contents coupled with impaired activities of antioxidant enzymes and free radical scavengers mirrored a situation of exacerbated testicular oxidative imbalance and disrupted redox homeostasis. FHPD, by and large, countermanded testicular steroidogenesis and antioxidant defence system and revoked the ill effects of arsenic. We conclude that specific protein-enriched diet may serve as prospective weaponry in encountering the arsenic-threatened testicular functions.

KEYWORDS

Arsenic, casein and pea, DNA damage, spermatozoa, ultrastructure

1 | INTRODUCTION

Arsenic is a ubiquitously existing environmental toxicant (IARC, 2004; WHO 2000). Adverse health consequences of arsenicosis have been a pressing global concern. Arsenic is often found in the air, water and soil; however, human exposure to arsenic primarily occurs through intake of polluted drinking water (NRC, 1999; Smith, Lopipero, Bates, & Steinmaus, 2002; Watanabe et al., 2003). In arsenicosis, risks of various cancers and noncancer illnesses including reproductive and developmental crises (Abernathy et al., 2003; NRC, 1999, 2001; Wasserman et al., 2004; Watanabe et al., 2003) are of grave concern to humans. Several laboratory models might help to understand the varied disease outcomes in arsenicosis. Nevertheless, our understanding of the arsenic-induced reproductive and developmental toxicity as yet remains deficient, and the causal associations amid laboratory versus. human vulnerability need to be ascertained.

In males, compromised testosterone production, apoptosis and necrosis seem accountable for the arsenic-induced gonadal dysfunction (Davila-Esqueda et al., 2012; Shen et al., 2013). Epidemiologic studies demonstrated that arsenic exposure might deteriorate sperm quality, cause erectile dysfunction and induce

 © 2020 Blackwell Verlag GmbH

Check for updates

Unsolicited Review

HET

Human and Experimental Toxicology
1–14
© The Author(s) 2021
Article reuse guidelines:
sagepub.com/journals-permissions
DOI: 10.1177/09603271211021474
journals.sagepub.com/home/het
SAGE

Molecular perspective concerning fluoride and arsenic mediated disorders on epididymal maturation of spermatozoa: A concise review

Priyankar Pal, Sagnik Biswas and Prabir Kumar Mukhopadhyay

Abstract

Epididymis is a complex tubular structure of male reproductive system where spermatozoa undergo maturation and gain the fertilizing ability. Epididymal pseudostratified columnar epithelium with different cell types play imperative role by their secretory properties and enrich the luminal microenvironment necessary for achieving spermatozoal motility. During epididymal transit several secretory proteins like P26h, SPAG11, HSPD1 and many others are deposited on spermatozoal surface. At the same time spermatozoal proteins are also modified in this intraluminal milieu, which include cyritestin, fertilin, CE9 and others. Natural and anthropogenic activities disclose various environmental pollutants which affect different physiological systems of animals and human being. Likewise, reproductive system is also being affected. Fluoride causes structural alterations of caput and cauda segments of epididymis. Redox homeostasis and functional integrity are also altered due to diminished activities of SOD1, GR, Crisp2, Lrp2 and other important proteins. On the contrary arsenic affects mostly on cauda segment. Redox imbalance and functional amendment in epididymis have been observed with arsenic revelation as evidenced by altered genomic appearance of SOD, GST, catalase, Ddx3Y, VEGF and VEGFR2. This review is dealt with structure-function interplay in normal epididymal spermatozoal maturation along with subsequent complications developed under fluoride and arsenic toxicities.

Keywords

Epididymis, spermatozoal maturation, reprotoxicity, fluoride, arsenic

Introduction

Spermatogenesis is exclusively dependent on close liaison in-between Sertoli and Leydig cells of testis.[1] However, the spermatozoa formed by the testis are immature and infertile.[2,3] The spermatozoa need to be transported via epididymis to mature entirely and thus attain the competence to fertilize.[4,5] The epididymis is sustained by an array of homeostatic control systems operated by hormonal and non-hormonal features, which coalesce to ensure spermatozoal maturation and fortification. It is a unique and fascinating accessory sex organ of the male reproductive system made up of super coiled and convoluted tubule restraining a nutritious luminal fluid required by the spermatozoa for the attainment of fertility.[6,7] Structural orientation has sub-divided epididymis into three different regions like caput, corpus and cauda.[6] They are composed of various types of cells which in turn by their secretory activities help to create and maintain the luminal fluid composition for spermatozoal nourishment.[7] The cauda portion of the epididymis stores the matured spermatozoa and also plays an active role in spermatozoal nutrition and transportation. Thus, epididymal maturation of spermatozoa is

Department of Life Sciences, Presidency University, Kolkata, West Bengal, India

Corresponding author:
Prabir Kumar Mukhopadhyay, Department of Life Sciences, Presidency University, 86/1 College Street, Kolkata 700073, West Bengal, India.
Email: prabir.dbs@presiuniv.ac.in